

**STUDY THE EFFECT OF CASTING SPEED,
SUPERHEAT AND MOULD ON
RHOMBOIDITY IN BILLETS**

By

ROHIT MISHRA

Management Trainee (Technical) 2011 Batch

P. No. 156993

Guided by

Mr. RAJIV BANKA



TATA STEEL LIMITED

JAMSHEDPUR

MARCH - APRIL 2012

ACKNOWLEDGEMENT

At this momentous occasion of completion of my project binding, I would like to acknowledge the contribution of all those benevolent people I have been blessed to associate with. Behind every project, there stand a myriad of people whose help and contribution makes things successful.

I am deeply indebted to my guide Mr. Rajiv Banka, Manager, LD#1 and for giving me an opportunity to work with him on this project. His advice and guidance throughout this work has been of immeasurable help not only in research work, but also in my development as a whole. I would like to specially thank Mr. E.Z. Chacko, Sr. Manager, TGGWL for his continual input and help in analysis. I want to take this opportunity to thank the Mr. D.K. Singh and other staffs of the Physical Laboratory and Metallography Laboratory under Scientific Services for their help in this project. Nevertheless, I am grateful to Mr. Debasis Das, Chief, LD#1 for providing a conducive and friendly atmosphere.

Last but not the least, I would like to express my deepest gratitude to the Almighty without his blessings, this project would not have been even half as much interesting or fun as it has been.

Date: April 27, 2012

Place: Jamshedpur

(Rohit Mishra)

EXECUTIVE SUMMARY

Rhomboidity in billets was investigated in this industrial study on CC3 billet caster at LD#1. This study focuses on events leading to variability in severity of rhomboidity. The effect of casting speed, superheat and mould design on severity of rhomboidity was evaluated. Based on the knowledge of the rhomboidity generated in this study, recommendations are proposed to minimize the problem.

The study was only focussed on TMT grade of steel. It was shown that at high casting speeds mainly above 3.5 m/min, severity of rhomboidity was high due to thin shell formation at the mould exit. The effect of superheat was not clear on rhomboidity. No specific trend or relation was been able to establish. During investigation of rhomboid billets occurrence in FY 2011-12, it was learned that cases of rhomboidity had surged from September'11 onwards. It was found out that different mould (Convex-2) was supplied by Concast instead of Convex type. The mould taper of Convex-2 is less in comparison with Convex type due to which heat transfer is low and hence shell formation at mould exit is thinner. Moreover, the sulphur print obtained for the billet casted with Convex-2 mould revealed re-entrant corners suggesting formation of air gap. Sulphur printing technique was used to study the shell formation in both the moulds.

TABLE OF CONTENTS

Acknowledgement.....	i
Executive Summary.....	ii
List of Figures.....	v
List of Tables.....	viii
Chapter 1: INTRODUCTION.....	1
Chapter 2: LITERATURE REVIEW.....	4
2.1 Moulds.....	4
2.1.1 Billet Casting Moulds.....	5
2.1.2 Bloom Casting Moulds.....	6
2.1.3 Slab Casting Moulds.....	6
2.1.4 Mould Taper.....	7
2.2 Heat Transfer in the Mould.....	7
2.2.1 Mould Midfaces.....	8
2.2.2 Mould Corners.....	9
2.3 Mould Thermal Response.....	9
2.4 Mould Distortion.....	10
2.5 Billet Solidification.....	11
2.5.1 Solid Shell Formation in the Mould.....	11
2.5.2 Cast Structure.....	12
2.6 Rhomboidity in Billets.....	14
Chapter 3: PLANT INDUCTION.....	17
3.1 Overview of LD#1.....	17

3.1.1	Supporting Facilities at LD#1.....	18
3.2	Details of the Billet Casters.....	19
3.3	Moulds used at CC3 in LD#1.....	21
3.3.1	Comparison of Conventional and Convex Moulds.....	22
3.3.2	Convex Type Mould.....	23
Chapter 4: SCOPE AND OBJECTIVES.....		25
Chapter 5: EXPERIMENTAL SETUP AND PROCEDURE.....		26
5.1	Casting Machine and Operation Practices.....	26
5.1.1	Experimental Casting Parameters.....	26
5.2	Details of Plant Trails.....	26
5.3	Billet Sample Preparation.....	28
5.4	Sulphur Printing (Baumann Method)	28
5.4.1	Principle.....	28
5.4.2	Procedure.....	28
5.5	Plant Trail Difficulties.....	29
Chapter 6: RESULTS AND DISCUSSION.....		30
6.1	Effect of Casting Speed on Rhomboidity.....	30
6.2	Effect of Superheat on Rhomboidity.....	36
6.3	Effect of Mould on Rhomboidity.....	37
6.3.1	Mould Taper and Section Size.....	38
6.3.2	Solid Shell Formation in Convex and Convex-2 Type Mould.....	39
6.4	Mechanism of Generation of Rhomboidity.....	46
Chapter 7: CONCLUSION.....		48
Chapter 8: WAY FOWARD.....		49
References.....		50

LIST OF FIGURES

Figure 1.1: Schematic of continuous casting

Figure 2.1: A mould tube.

Figure 2.2: Cross sectional view of mould jacket.

Figure 2.3: Top view of billet casting mould tube.

Figure 2.4: Top view of bloom casting mould tube.

Figure 2.5: Top view of slab casting mould tube.

Figure 2.6: Schematic representation of thermal resistance to heat flow.

Figure 2.7: Typical mould midface heat transfer profiles for 0.05 and 0.7 wt%C grades cast at 1.3m/min

Figure 2.8: A schematic of the dynamically distorted mould is shown through the thickness of the mould wall to illustrate dynamic tapers. A steep negative taper forms above the peak distortion, followed by a positive taper, allowing mould-strand interaction to occur during the mould oscillation. (Not to scale)

Figure 2.9: Solidified shell obtained from controlled breakouts for steels with 0.0 to 0.90% carbon

Figure 2.10: Billet section showing reentrant corners.

Figure 2.11: Transverse section of billet showing formation of air gap.

Figure 2.12: Schematic diagram showing a billet with non-uniform solid shell thickness being distorted into rhomboid shape by spray cooling.

Figure 2.13: Effect of mould taper on rhomboidity for range of carbon content in steel billets.

Figure 3.1: Layout of LD Shop #1.

Figure 3.2: Top view of Convex type mould.

Figure 3.3: Longitudinal view of Convex type mould and its taper at both midface and corner.

Figure 6.1: Variation in rhomboidity with casting speed for Strand 1 at CC3.

Figure 6.2: Variation in rhomboidity with casting speed for Strand 2 at CC3.

Figure 6.3: Variation in rhomboidity with casting speed for Strand 3 at CC3.

Figure 6.4: Variation in rhomboidity with casting speed for Strand 4 at CC3.

Figure 6.5: Variation in rhomboidity with casting speed for Strand 5 at CC3.

Figure 6.6: Variation in rhomboidity with casting speed for Strand 6 at CC3.

Figure 6.7: Variation in rhomboidity with different ranges of superheat at CC3.

Figure 6.8: Number of rhomboid billets from CC3 in FY 2011-12 (strandwise).

Figure 6.9: Mould profile and taper of curved side for Convex and Convex-2 moulds.

Figure 6.10 (a to n): Sulphur prints of billet casted by Convex-2 mould at different distances from the mould entry

Figure 6.11(a to j): Sulphur prints of billet casted by Convex mould at different distances from the mould entry

Figure 6.12: Solid shell formation profile for midfaces of Convex mould on curved side

Figure 6.13: Solid shell formation profile for midfaces of Convex-2 mould on curved side

Figure 6.14: Solid shell formation profile for corners of Convex mould on curved side

Figure 6.15: Solid shell formation profile for corners of Convex-2 mould on curved side

Figure 6.16: Stresses over solid shell at the exit of the mould

LIST OF TABLES

Table 3.1: Details of three casting machines at LD#1.

Table 3.2: Different Moulds used at CC3, LD#1.

Table 3.3: Comparison of Conventional and Convex Moulds.

Table 5.1: Plant Trail Details.

Table 6.1: Casting speed and rhomboidity for Strand 1.

Table 6.2: Casting speed and rhomboidity for Strand 2.

Table 6.3: Casting speed and rhomboidity for Strand 3.

Table 6.4: Casting speed and rhomboidity for Strand 4.

Table 6.5: Casting speed and rhomboidity for Strand 5.

Table 6.6: Casting speed and rhomboidity for Strand 6.

Table 6.7: Superheat and rhomboidity for CC3.

INTRODUCTION

Continuous casting, also called strand casting, is the process whereby molten metal is solidified into a "semi finished" billet, bloom, or slab for subsequent rolling in the finishing mills. Prior to the introduction of continuous casting in the 1950s, steel was poured into stationary moulds to form ingots. Since then, "continuous casting" has evolved to achieve improved yield, quality, productivity and cost efficiency. It allows lower-cost production of metal sections with better quality, due to the inherently lower costs of continuous, standardized production of a product, as well as providing increased control over the process through automation.

Molten metal (known as hot metal) is tapped into the ladle from furnaces. After undergoing any ladle treatments, such as alloying and degassing, and arriving at the correct temperature, the ladle is transported to the top of the casting machine. Usually, the ladle sits in a slot on a rotating turret at the casting machine; one ladle is 'on cast' (feeding the casting machine) while the other is made ready, and is switched to the casting position once the first ladle is empty.

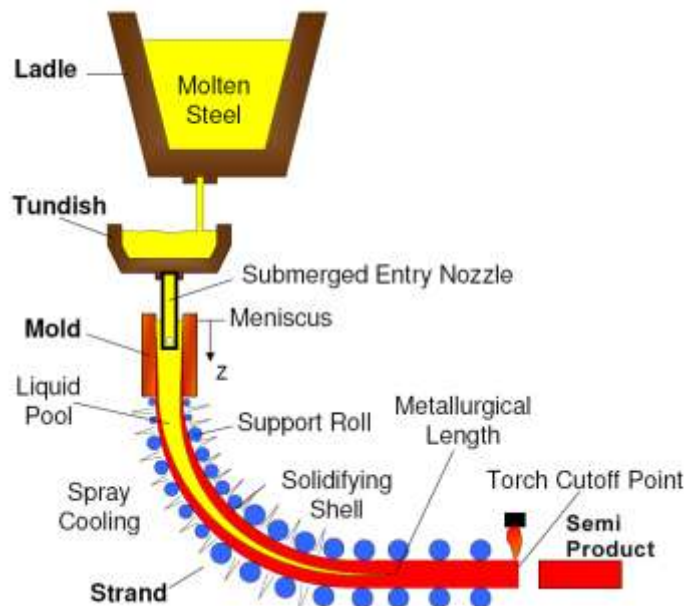


Fig. 1.1: Schematic of continuous casting

From the ladle, the hot metal is transferred via a refractory shroud to a holding bath called a tundish. The tundish allows a reservoir of metal to feed the casting machine while ladles are switched, thus acting as a buffer of hot metal, as well as smoothing out flow, regulating metal feed to the moulds and cleaning the metal.

Metal is drained from the tundish through another shroud into the top of an open-base copper mould. The depth of the mould can range from 0.5 to 2 meters, depending on the casting speed and section size. The mould is water-cooled to solidify the hot metal directly in contact with it; this is the primary cooling process

In the mould, a thin shell of metal next to the mould walls solidifies before the middle section, now called a strand, exits the base of the mould into a spray-chamber; the bulk of metal within the walls of the strand is still molten. The strand is immediately supported by closely spaced, water cooled rollers, these acts to support the walls of the strand against the ferrostatic pressure of the still-solidifying liquid within the strand. To increase the rate of solidification, the strand is also sprayed with large amounts of water as it passes through the spray-chamber; this is the secondary cooling process. Final solidification of the strand may take place after the strand has exited the spray-chamber.

Billet rhomboidity (or off-squareness) which is defined as the difference between the lengths of the two diagonals, has been a major quality problem since the inception of continuous casting. The absolute value of the difference is a measure of severity of rhomboidity while sign (positive or negative) associated with the measured value is indicative of the orientation of rhomboidity. It is also common for the magnitude and orientation of rhomboidity to change with time in the heat and sometimes “twisting” of billets on cooling bed is observed. With respect to severity of problem many mills consider a difference in diagonals of greater than ~ 8 mm unacceptable because the rhomboid billet causes processing difficulties in the reheat furnace and subsequent hot rolling operations. Furthermore, billets with excessively large rhomboidity can crack along the diagonal or the corners.

A large rhomboidity obviously suggests lack of control and the presence of non-uniform cooling conditions in the mould and/or sprays. In the mould, heat transfer is related to thermo-mechanical behaviour of the mould and the nature of mould-strand interaction.[1] The behaviour of meniscus which is affected by metal level fluctuation is another critical variable that can influence heat transfer and progress of solidification, leading to non-uniform shell thickness and oscillation marks of variable depth. Thus rhomboidity is affected by a number of mould designs, operating variables and process upsets.

The information presented in literature provides useful insights on generation of rhomboidity. For example, the effect of steel carbon content on the severity of rhomboidity is quite important; it was reported that steel grades with carbon content in the ~ 0.17 to 0.45 percent range are more sensitive to the problem than others.[2-4] Another important parameter is the mould taper at the

meniscus level. The parabolically and double tapered moulds generally have steeper taper (in excess of $\sim 2.0\%/m$) in the meniscus region and low heat transfer while single tapered moulds have shallow tapers ($\sim 0.8\%/m$) and high heat transfer.[1] Even flow of lubricating oil plays a role in rhomboidity generation. In earlier studies on rhomboidity in billets,[5-7] asynchronous boiling in the cooling water channel was identified as an important contributor. The region of the mould that is most affected by boiling is the area close to meniscus. It was shown mathematically that operating with low water velocity results in intermittent, asynchronous boiling on the four cold faces.

Other shape defects are namely, high section and bulging. High section is the increase in the billet cross sectional dimension occurred due to mould wear at the mould exit. Bulging mainly occurs due to low shell thickness at the mould exit, occurrence of re-entrant corners and excess pressure at withdrawal unit.

LITERATURE REVIEW

This chapter provides the necessary background for understanding of heat transfer, billet solidification, mould-strands interaction and effects of various parameters on shape defects, mainly rhomboidity.

2.1 Moulds

The mould is the heart of the continuous casting machine in many respects. Being primary heat extraction device, it is required to solidify a shell of sufficient thickness to contain the liquid core in the sub-mould region. The mould also provides support to the newly solidified shell at the time when the shell is weak and susceptible to bulging due to ferrostatic pressure. The surface quality, shape and even the internal quality of the solidified steel is profoundly by the design and operation of the mould.

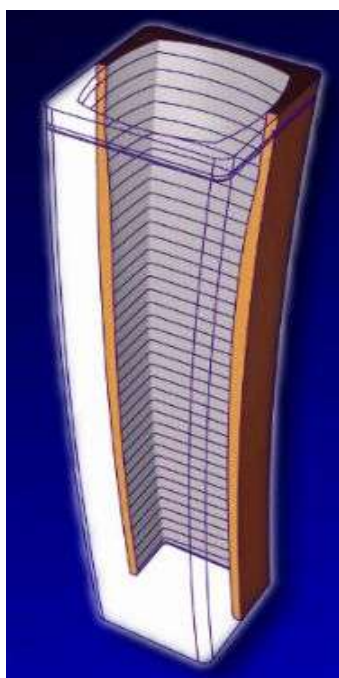


Fig.2.1: A mould tube

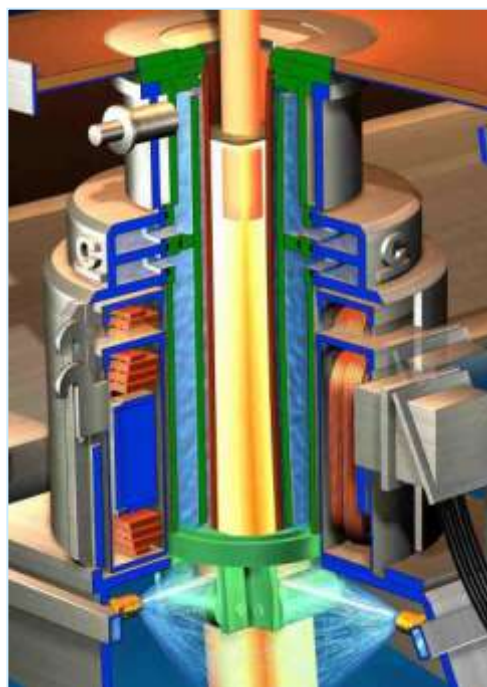


Fig.2.2: Cross sectional view of mould jacket

As the molten steel enters the mould, heat is extracted & a solid steel shell forms. The molten steel will be formed into certain shape steel billets/slabs immediately after passing through the mould. Situated in the critical position of continuous casting mould tube requires extreme high conductivity & high strength. Beside basic function of shaping & solidifying the steel strand, copper mould tube is of great influence on the economics of continuous casting lines. Not only

are the cost, service life of copper mould tube & quality of cast product also an important factor. Thus suitable mould design is necessary to be chosen for the economics of continuous casting.

Mould tube requires complex design due to shrinkage occurs in steel during solidification. Any material when transforms from liquid to solid state, then shrinkage in size will take place. Thus shrinkage is the main reason for the complex design of mould. During solidification process the steel shrinks, hence to maintain contact between the mould & the solidifying steel, the cross section exit of the mould is made slightly smaller than the top of the mould. This feature is known as Mould Taper. Thus, taper is the reduction in inside cross-section from top to bottom.

There are three basic types of mould used in continuous casting:

These are:

1. Tube Mould: Billets Casting
2. Plate Mould: Bloom Casting
3. Plate Mould with adjustable width: Slab Casting

2.1.1 Billet Casting Moulds

In Billet Casting tube mould is used which is made up of copper along with some other alloying elements in small amounts. These tube varies from 0.5M in length to 2M in length. These tubes are fixed in the mould jacket. Mould Jacket consists of precise gap & different chambers for inlet & outlet water flow. It also contains seal O'ring which ensures that water will not come out of the jacket.



Fig. 2.3: Top view of billet casting mould tube

2.1.2 Bloom Casting Moulds

Bloom Casting Moulds are generally plate's type construction, but with no facilities for in cast strand dimensional changes as in case of Slab casting. Its taper is fixed, dependent on the section size & created by appropriate machining of the plates.



Fig.2.4: Top view of bloom casting mould

2.1.3 Slab Casting Mould

Slab Casting Mould is made of steel frame and consists of two wide plates and two narrow plates. These plates are made of copper. Mould width is adjustable as per requirement. Mould width is being changed with the help of four gear boxes, electrical motor, and encoder. Each side of end plate is connected by two gear box one at top and another at bottom. By giving command for width changing, these gear boxes take drive from electrical motor and gives the required width. This type of mould is made with on line and off line width changing. Thus changing the dimensions of the slabs are easy in this type of casting.

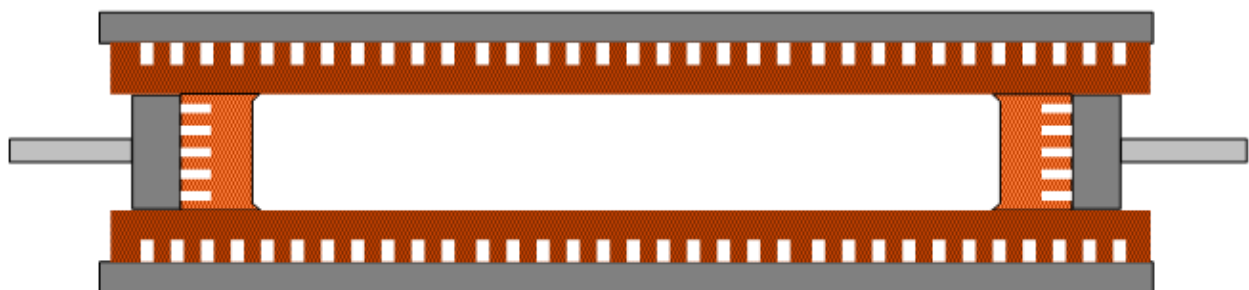


Fig.2.5: Top view of slab casting mould

Slab casting mould is equipped with thermocouples. These thermocouples are interfaced to a personal computer system along with other key casting parameters like casting speed. The

Computer evaluates in real time output from the thermocouples to provide sticker alarms & surface quality related operator advice. It helps in evaluating following data:

1. Detection of sticker types breakouts
2. Detection of substandard casting conditions, asymmetric flow etc to predict surface cracks & other type of breakouts etc.

2.1.4 Mould Taper

Taper is the reduction in cross section size from one end. Every suppliers design a particular type of taper for copper tube depending upon its own findings and measurement. Taper is the measure of profile of a copper tube. It is measured by the unit %/meter. A probe is run down the inside of the tube that measures the wall to wall distance along the length. Taper is calculated as follows

$$\text{Taper} = [(\text{Wall to wall distance at the top} - \text{Wall to wall distance at the bottom}) / \text{Wall to wall distance at the top}] / \text{Length}$$

Taper is necessary in the mould design to maintain contact between the solidifying steel & the mould wall. If the contact between the mould wall & the solidifying steel is not there, then air gap will occur due to reduction in the cross section size of the steel & thus heat transfer problem will occur. Heat transfer is very less in air medium in comparison to other medium of heat transfer present in the mould during casting.

The taper designs are:

1. Single Taper
2. Double Taper
3. Multi Taper
4. Parabolic Taper
5. Funnel at the top region

2.2 Heat Transfer in the Mould

Heat transfer from the strand surface is transferred to the mould cooling water by a sequence of steps in series. As shown in Figure 2.6, these consist of^[1]:

- (i) Conduction and radiation across an air gap separating the mould and the strand
- (ii) Conduction through the mould wall itself
- (iii) Convection at the mould/ cooling water interface.

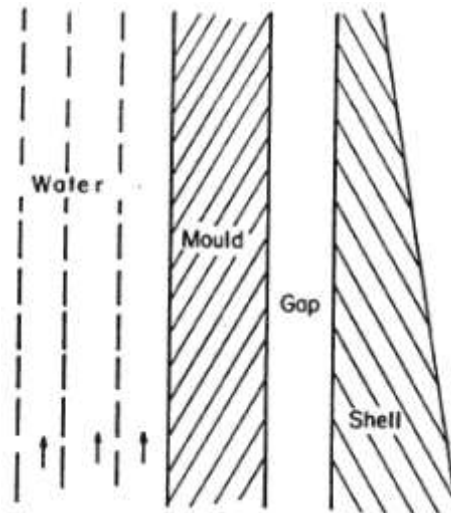


Fig.2.6: Schematic representation of thermal resistance to heat flow^[1]

It was found that the air gap constitutes the largest resistance, being 84% of the total, while the mould wall and mould/ cooling water interface accounted for only 2 and 14%, respectively. Thus, the pattern of heat removal in the mould is dependent largely on the dynamics of gap formation^[1].

The gap is formed through simultaneous contraction of the solidifying shell and the thermal distortion of the mould walls, and it is inhibited by the ferrostatic pressure of the liquid core^[9]. Furthermore, the size of the gap is constantly changing in response to the local dynamics of the mould. Therefore, any variables which affect the dynamics and properties of the air gap will have profound impact on the heat transfer response of the mould. Generally the size of the air gap increases with distance down the mould due to solidification shrinkage and mould distortion. Therefore, the hot face heat transfer is greatest near the meniscus and decreases in magnitude down the mould. The heat transfer profile is also not uniform across the transverse face of the mould due to physical differences in the corner geometry, as well as two dimensional heat flows at the corners.

2.2.1 Mould Midfaces

At the midface of the mould, the maximum heat transfer occurs about 25 to 40 mm below the meniscus for carbon grades up to 0.8 wt%C^[5,6,10]. Typical heat transfer profiles for high and low

carbon grade steels can be seen in Figure 2.7, for a casting speed of 1.3 m/min. The effect of carbon content and casting speed will be discussed later.

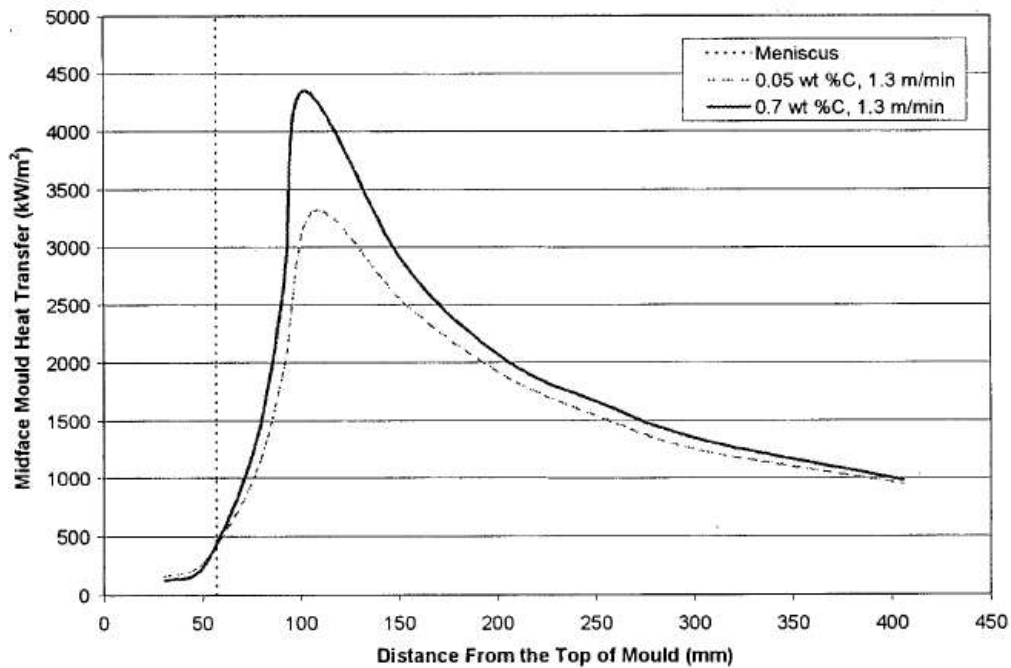


Fig. 2.7: Typical mould midface heat transfer profiles for 0.05 and 0.7 wt%C grades cast at 1.3m/min^[10]

2.2.2 Mould Corners

The mould corners are inherently more rigid than the midfaces of the mould. The corner region in the mould is cooler than midface due to its rigidity and the two dimensional heat flow, which generates more shrinkage and a larger gap between the strand and the mould^[5]. Consequently, the heat transfer is lower at the corners of the mould.

Blazek^[10] had conducted laboratory scale trails which suggested than the heat transfer at the corners were 30 to 40% lower than that at the midfaces of the mould at a casting speed of 1.3m/min.

2.3 Mould Thermal Response

The thermal profile of the mould is determined by the heat transfer characteristics in the mould. The thermal profile of the mould wall, in effect, results as a combination of the heat transfer from the strand through the mould-strand gap to the mould wall, conduction through the mould

wall, and the heat extracted by the cooling water. The thermal response of the mould is highly influenced by the heat transfer from the strand, lubricant type and properties, mould taper, mould wall thickness and mould material. The thermal profile of the mould generally flows same behaviour as that of heat transfer. The mould temperature reaches a peak around 30 to 40 mm below the meniscus level^[5,6,9]. Below this region, the temperatures decrease due to solidification of the shell, which act to increase both the mould-strand gap and the total conductive resistance of the heat flow circuit. As well, the stronger and thicker shell is more able to withstand the ferrostatic pressure which would ordinarily aid reducing the air gap. Furthermore, the thermal standard deviations temperature profiles are greatest at the meniscus and relatively small for the remainder of the mould.

2.4 Mould Distortion

Mould distortion results from thermal expansion and mechanical bending of the mould walls during casting. Mould distortion is a dynamic event, which may result in structural damage to the mould, through permanent distortion of the mould walls. Thermal stresses are generated as a result of the dynamic distortion of the mould wall. Permanent distortion of the mould wall will occur if these stresses exceed the local hot yield stress of the mould material at any point in the distorted region^[5].

Distortion also occurs at the mould corner, and is larger than at the midfaces due to the triaxial state of stress. Furthermore, the distortion is not necessarily symmetrical at each corner junction. The region of distortion is described in terms of a dynamic negative taper, which forms above the peak distortion, and a dynamic positive taper, which forms below (Figure 2.8). These taper are not static, but change dynamically with the mould temperature fluctuations that can result from intermittent nucleate boiling in the water channel or metal level turbulence.

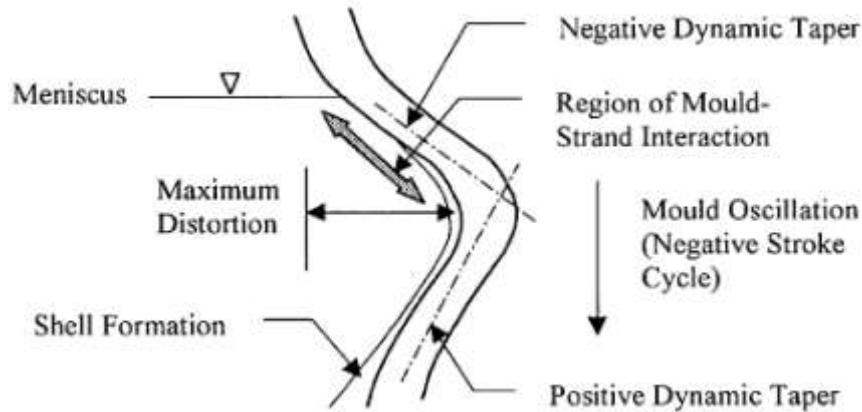


Fig.2.8: A schematic of the dynamically distorted mould is shown through the thickness of the mould wall to illustrate dynamic tapers. A steep negative taper forms above the peak distortion, followed by a positive taper, allowing mould-strand interaction to occur during the mould oscillation. (Not to scale)

2.5 Billet Solidification

Solidification events in the mould and sub-mould regions directly influence strand quality and, to some extent, the productivity and yield of the casting operation.

2.5.1 Solid Shell Formation in the Mould

A minimum shell thickness is necessary at the mould exit to withstand the ferrostatic pressure in the liquid core. Theoretically, the shell thickness at the mould exit is proportional to the dwell time of the casting in the mould. However, shell formation in the mould is rarely uniform but varies in both transverse (i.e. re-entrant corners) and longitudinal (wavy shell formation due to δ to γ transformation) directions. Shell formation depends on steel compositions, superheat, fluid flow conditions in the mould due to nozzle design or electromagnetic stirring, mould lubrication and mould design. Any localized thinning of the shell due to these variables may result in surface cracks or breakouts. Thus the casting speed must be limited to ensure that the thinnest portion of the solid shell at mould exit can withstand the stresses induced by the ferrostatic pressure.

Singh and Blazek studied the influence of steel chemistry on shell formation through series of controlled breakout experiments and found the shell profile to be dependent on steel carbon content (Figure 2.9). Below 0.40%C, the shell thickness fluctuates in the longitudinal direction, whereas at higher carbon contents, the shell thickness increases steadily with distance below the meniscus^[10].

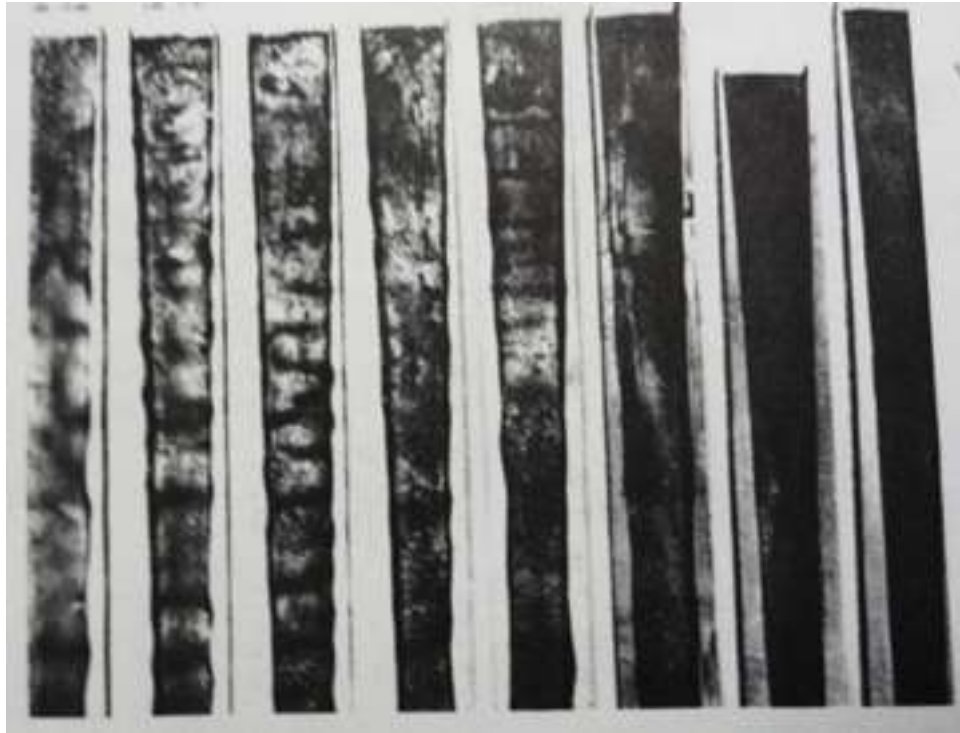


Fig.2.9: Solidified shell obtained from controlled breakouts for steels with 0 to 0.90% carbon^[10]

Grill and Brimacombe^[11] have proposed that the wavy shell formation results from stresses arising from the δ to γ phase transformation. At 0.1%C, steel experiences the maximum δ to γ phase transformation in solid state than higher carbon steels.

Shell thickness may also vary in the transverse directions. One characteristic feature is the localized thinning in the corner regions of the cast section, Figure 2.10, normally referred to as re-entrant corners. Re-entrant corners form as a result of the complex behaviour of the air gap between the solidified strand and the mould wall. An air gap first forms at the corners where the cooling is most rapid due to two dimensional heat flow. Once formed, the gap reduces the rate of heat transfer so solidification is retarded at the corners^[12]. As time progresses (with increasing distance below the meniscus) the gap spreads from the corners to the midface of the strand, but the gap width is less at the midface than at the corners due to bulging caused by ferrostatic pressure.

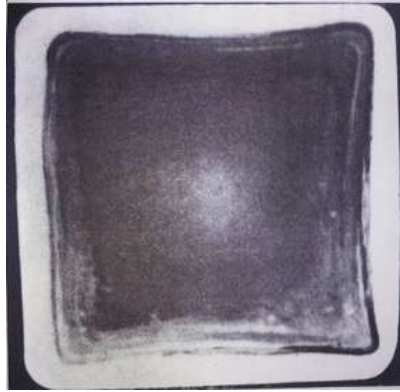


Fig.2.10: Billet section showing reentrant corners^[12]

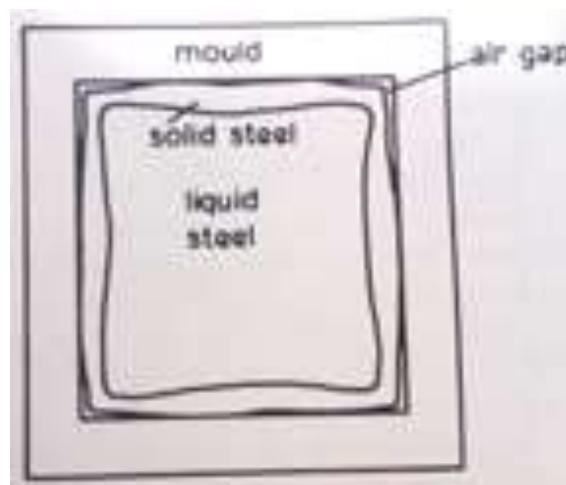


Fig.2.11: Transverse section of billet showing formation of air gap^[12]

2.5.2 Cast Structure

The cast structure consists of three zones^[1]:

- (i) A chill zone adjacent to the strand surface where the structure consists of fine equiaxed crystals
- (ii) A columnar zone in which dendrites extend inward from chill zone, perpendicular to strand surface
- (iii) A central equiaxed zone which consists of randomly oriented dendrites

The relative size of the central equiaxed zone and columnar zone are of primary concern when investigating internal quality. Columnar dendrites are more susceptible to the formation of internal cracks than the equiaxed dendrites, and a long columnar zone increases the severity of centreline segregation and porosity. The relative size of equiaxed and columnar zones depend on

steel superheat, machine design, section size, flow conditions on the liquid pool and steel chemistry.

2.6 Rhomboidity in Billets

Billet rhomboidity (or off-squareness) which is defined as the difference between the lengths of the two diagonals, has been a major quality problem since the inception of continuous casting. The absolute value of the difference is a measure of severity of rhomboidity while sign (positive or negative) associated with the measured value is indicative of the orientation of rhomboidity. It is also common for the magnitude and orientation of rhomboidity to change with time in the heat and sometimes “twisting” of billets on cooling bed is observed. With respect to severity of problem many mills consider a difference in diagonals of greater than ~ 8 mm unacceptable because the rhomboid billet causes processing difficulties in the reheat furnace and subsequent hot rolling operations. Furthermore, billets with excessively large rhomboidity can crack along the diagonal or the corners.

A large rhomboidity obviously suggests lack of control and the presence of non-uniform cooling conditions in the mould and/or sprays. In the mould, heat transfer is related to thermo-mechanical behaviour of the mould and the nature of mould-strand interaction^[7]. The behaviour of meniscus which is affected by metal level fluctuation is another critical variable that can influence heat transfer and progress of solidification, leading to non-uniform shell thickness and oscillation marks of variable depth. Thus rhomboidity is affected by a number of mould designs, operating variables and process upsets.

The information presented in literature provides useful insights on generation of rhomboidity. For example, the effect of steel carbon content on the severity of rhomboidity is quite important; it was reported that steel grades with carbon content in the ~ 0.17 to 0.45 percent range are more sensitive to the problem than others.^[2-4] Another important parameter is the mould taper at the meniscus level. The parabolically and double tapered moulds generally have steeper taper (in excess of $\sim 2.0\%/m$) in the meniscus region and low heat transfer while single tapered moulds have shallow tapers ($\sim 0.8\%/m$) and high heat transfer.^[1] Even flow of lubricating oil plays a role in rhomboidity generation.

In earlier studies on rhomboidity in billets,^[5-7] asynchronous boiling in the cooling water channel was identified as an important contributor. The region of the mould that is most affected by boiling is the area close to meniscus. It was shown mathematically that operating with low water

velocity results in intermittent, asynchronous boiling on the four cold faces. When boiling occurs, the cold face temperature of the mould strongly influences the instantaneous rate of heat removal by cooling water such that the mould wall temperature on a given face can fluctuate out of control^[5-7]. When the water velocity is reduced, boiling on the four cold faces becomes more vigorous and less intermittent such that the cooling around the billet periphery becomes more uniform.

Another mechanism proposed to explain generation of rhomboidity based on oscillation mark formation and non-uniform heat transfer in mould and the sprays. The problem begins with the formation of deep and non-uniform oscillation marks around the billet periphery. In the vicinity of a deep oscillation mark, the rate of heat removal is low due to mould-strand gap. On the other hand, regions of the billets having shallow oscillation marks experience higher rates of heat extraction. Thus, the presence of non-uniform oscillation marks on the billet surface gives rise to markedly difference in heat extraction leading to non-uniform solid shell. Thus, the billet exiting mould, although reasonably square, has non-uniform solid shell, as shown in Figure 2.12 which is a schematic representation of this concept. In the sprays, the colder portions of the strand, having thicker solid shell, tend to cool faster than the hotter regions because of the effect of unstable boiling; the result is non-uniform shrinkage of the billet and rhomboidity. During casting process following are observed:

- (a) The obtuse-angle corners of rhomboid billet have been found to have deepest oscillation marks^[13].
- (b) The billets emerging from the mould, when observed through peep-hole, showed that, of the two corners in view, one was cold (dark) and the other was hot (bright). Subsequent inspection of billets on cooling bed indicated that acute-angle corners in billet correspond to the colder corners whereas the hot corners formed the obtuse angle of the billet^[13].

Occasionally, billets on the cooling bed are found to be twisted. This indicates that magnitude and orientation of rhomboidity varies along the length of the billet and this suggests that the event generating rhomboidity changes with time. It is possible that the root cause may lay in the mould such metal level fluctuation.

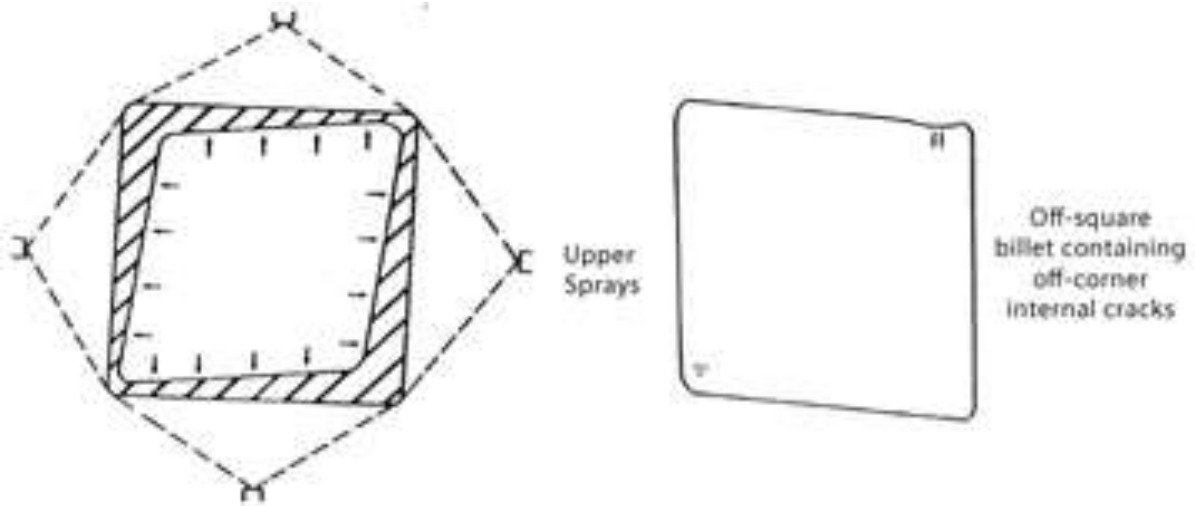


Fig.2.12: Schematic diagram showing a billet with non-uniform solid shell thickness being distorted into rhomboid shape by spray cooling^[9]

Another interesting aspect of rhomboidity is the effect of mould taper and steel grade (carbon content) on its severity as shown in Figure 2.13. With respect to the severity of rhomboidity, the graph indicates that parabolically tapered moulds are most effective followed by double tapered moulds while single tapered moulds are the worst^[2]. Furthermore, steel grades with carbon content in the range ~ 0.17 to $\sim 0.45\%$ are worse than other grades^[2]. From the work done by Brimacombe, Samarasekera and Kumar^[9], they suggested that rhomboidity is less in case of casting done by steep tapered mould in the meniscus region, as mould heat transfer for steep tapered mould is higher.

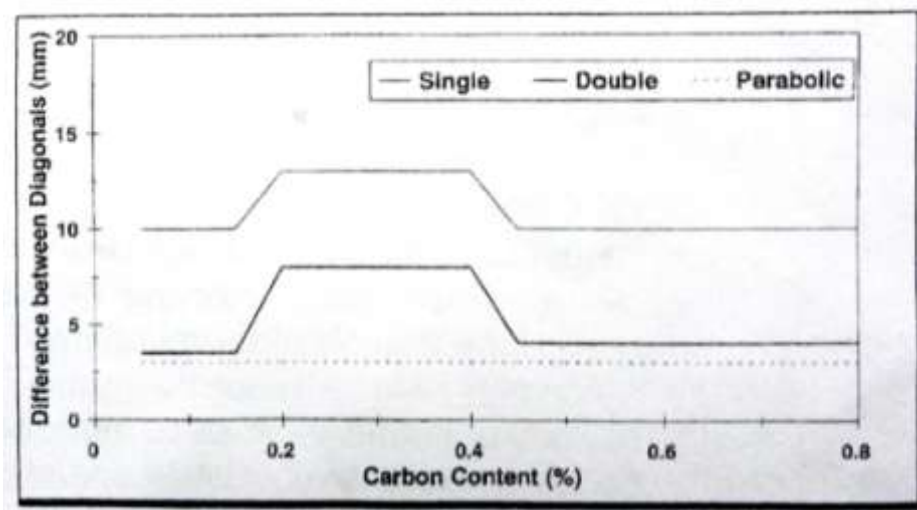


Fig.2.13: Effect of mould taper on rhomboidity for range of carbon content in steel billets

PLANT INDUCTION

3.1 Overview of LD#1

During modernization of SMS2 (steel melting shop) Tata Steel has established its first BOF (basic oxygen furnace) to meet the steel demand and for technological improvement in steel making. The Modernization Phase 1 Program of Rs. 220 crores, which basically updated the steel making facilities, marks an important milestone in the history of the Plant. The 29-month program was formally launched on Dec. 8, 1980, and it was completed in March 1983 with the commissioning of the 1.1 million tonnes per annum Basic Oxygen Furnace, i.e. L.D. Shop#1.

It has the following main features:-

1. Two numbers of 155 ton basic O₂ converters, with flux charging system, gas cleaning and gas recovery plant. Top blowing with six lance hole and bottom stirring with TBM (thyssen niederhhein blowing metallurgy). Supplier of Main Equipments: M/s Davy McKee, U.K. Electrical Equipment Supplier: M/s Bharat Heavy Electricals Ltd. (BHEL)
2. Basic refractories for Ladle
3. One 130 tonne Vacuum Arc Degassing and Refining (VADR) unit supplied by M/s Standard Messo, Duisberg and Westerwerke Project Limited for making special quality engineering steels such as CHQ,CSQ. Bbp teeming facilities for VADR heats
4. Three numbers of Ladle furnaces supplied by M/s SMS Demag.
5. Calcium injection treatment of Liquid steel.
6. Two Hot Metal De-sulphurisation Units with facility of mono-injection.
7. Ladle metallurgy stations for each caster equipped with top purging and Ca wire feeding
8. Basic [Dry vibratable mass] & deeper tundishes.
9. Ladle to Tundish shroud facility.
10. One six - strand continuous casting machine (Radius: 6 m) supplied by M/s Concast AG and Concast India with SEN/EMS facility. Cast Section: 130 mm². Equipped with Hard Cooling & Mould Stirrer established in 1983.
11. One six strand continuous casting machine (Radius: 9 m) supplied by M/s VAI Pomini. Cast Sections: 130 & 150 mm². Equipped with Hard Cooling & Mould Stirrer established in 1997.

12. One another six strand continuous casting machine (Radius: 9 m) supplied by M/s VAI Pomini. Cast Sections: 130 & 150 mm². Equipped with Hard Cooling, Mould Stirrer & SEN facility established in 2008.

3.1.1 Supporting Facilities at LD#1

1. Two 250 tonnes per day Oxygen Plants for supplying 99.5% pure O₂ for blowing in the converters. This plant has been supplied by M/s Cryoplants, U.K., and their Indian associates, Indian Oxygen Ltd.
2. Two 300 tonnes per day Lime Calcining Plants to provide quality flux for steel making. Engineering Projects India Ltd has supplied the limekilns of Maerz design.
3. One 18,000 tonne per annum Tar-Dolo Block plant to supply special refractories for lining the converters, along with a Dolo-sintering kiln. The equipment for the Dolo Block Plant has been imported from M/s Laeiswerke, West Germany.
4. The basic engineering and know-how for the Calcining of superior grade limestone for the production of high reactivity lime and sintering of high purity dolomite essential for the L.D. lining has been supplied by M/s Dolomitwerke, West Germany, the consultants for these two schemes.

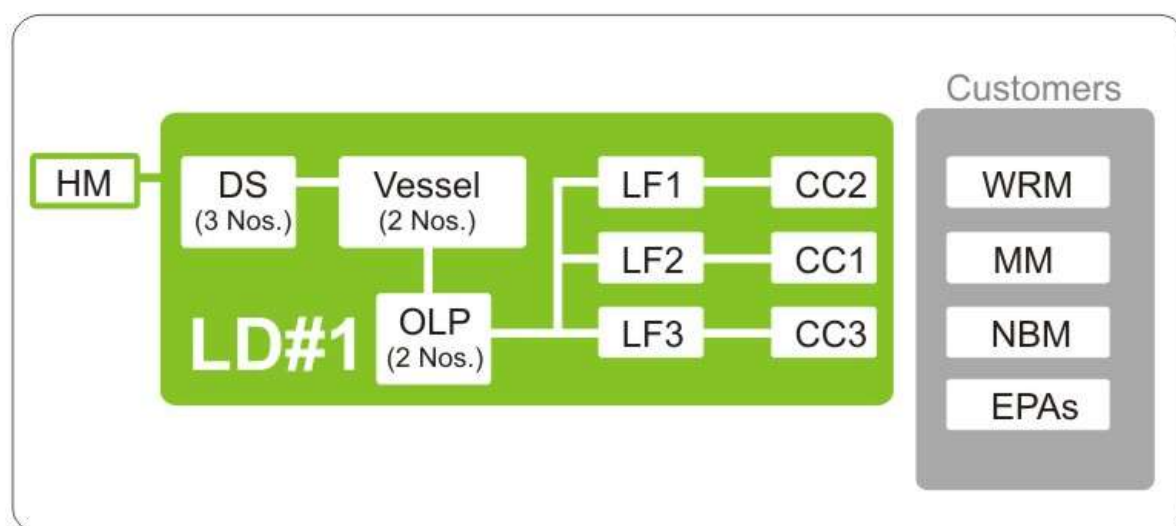


Fig.3.1: Layout of LD Shop #1

DS: Desulphurising Unit

OLP: Online Purging

MM: Merchant Mill

NBM: New Bar Mill

LF: Ladle Furnace

CC: Continuous Caster

WRM: Wire Rod Mill

EPAs: External Processing Agencies

3.2 Details of the Billet Casters

LD#1 has three 6-strand billet casters. The details of the casters are given in Table 3.1.

Table 3.1: Details of three casting machines at LD#1

Item		UOM	Plant		
			Jamshedpur – Longs		
			CC1	CC2	CC3
Machine	Make		Concast	Concast/VAIP	VAIP
	Start-up	year	1983	1997	3-Oct-08
	Upgradation (if any)	year	2002/2005	2005	-
	Caster type		Curved	Curved	Curved
	Metallurgical length	m	15.9	25.4	26.4
	Radius	m	6/11	9	9
	Section size	mm	130	130, 150	130, 150
	Strands	nos	6	6	6
	Interstrand distance	mm	1100	1100	1250
	Turret	Type	Butterfly - Fixed- TGS	Independent arm - Danieli	Butterfly - Fixed- TGS
	Tundish Car	Type	Semi-Cantilever	Semi-Cantilever	Full Canteilever
	Dummy Bar	Type	Rigid	Rigid	Rigid
	Cutoff	Type	Torch	Torch	Torch
	Length Measuring Device	Type	Encoder in Top roll of withdrawal	Encoder in Top roll of withdrawal	Encoder in Top roll of withdrawal
	Make of TCM	Type	Concast	Alba	Alba
	Pusher	Type	Single level	Double level	Double level
	Cooling Bed	Type	Hydraulic	Electr- Mechanical	Hydraulic
	Billet Marking	Type	Manual	Manual	Numtec – Stamping
	Max Casting Speed (130 mm sq)	M/min	3.4	3.8	4.4
	Present Capacity	million tons	0.8	1	1.1
	Capacity planned under next revamp	million tons	1 (FY '11)	1.2 (FY '11)	
Ladle	Heat size	t	150		
	Vortex breaker	Y/N	No		
	Slag detector	Y/N	No		
	Slide Gate	Make	LS-70		
	Slide gate control	Type	Manual		
	Lining	Type	Tar Dolo with Mag C slag zone		
	Porous Plug	Make	Vesuvius - IPV 2		
	Nozzle size	mm	65		
Tundish	Size	t	24	32	~ 34
	Shape	Type	Delta	Delta -T	Delta – T
	Covering type		Basic + Rice husk		
	Anti-vortex	Type	Impact pot flow modifier – Turbostop		
	Lining	Type	MgO dry powder		
	Casting Modes	Type	Open & Submerged	Open	Open & Submerged
	Nozzle Changer	Type	CNC- Vesuvius		
	Stopper Control	Type	Electro-Mech	None	Hydraulic

	Preheater	Type	CEBA	None	CEBA
	SEN	Type	Alumina C with zirconia band	NA	
Mould	Type	Type	Tube	Tube with slot (at region of radioactive source)	Tube with slot (at region of radioactive source)
	Mould Tubes Supplier	Make	Concast, Europa Metalli	Concast, Europa Metalli	Concast, Europa Metalli
	Mould Taper	Type	Parabolic, Convex	Parabolic, Convex	Parabolic, Convex
	Mould Material	Type	Convex - Cu Ag, EM -		
	Coating Material	Type	Chromium		
	Length	mm	900	1000	1000
	Life	Hours	250	150mm2 - 500, 130mm2 - 250	300
	Wall thickness	mm	13	150mm2 - 15 (11 at slot area), 130mm2 - 13 (9 at slot area)	150mm2 - 15 (11 at slot area), 130mm2 - 13 (9 at slot area)
	Water Channel gap	mm	3.5	4	4
	Inner jacket	Type	Self aligning with ribs	Fixed	Self aligning with buttons
	Max water flow	lpm	2200	2400	2400
	Operating flows	lpm	2000	1800 (130), 2100 (150)	2000 (130), 2200(150)
	Back Pressure	Bar			
	Foot Rolls	No.s	Single row	Single row	Single row
	Level Control	Type	Co60 – Berthold	Co60 - Berthold	Co60 – Berthold
	Machine start	Type	Automatic	Automatic	Automatic
	Lubrication	Type	Oil / Powder	Oil	Oil/Powder
	Type of Oil	Type	Rapeseed	Synthetic	Rapeseed
	Supplier of Casting Powder	Make	Stollberg	-	Stollberg
	Flux feeding	Type	Manual	NA	Manual
	Oscillation	Type	Electro-Mech	Hydraulic - Dynaflex	Hydraulic – Dynaflex
	Oscillation stoke	mm	3.4 - 4.1-5.2-6.4-7.6-8.8-9.8-10.8-11.5-12.5-12.7	Variable - 4 to 14 mm linked to casting speed	Variable - 4 to 14 mm linked to casting speed
	Oscillation Frequency	1/min	60 - 250 cpm linked to casting speed	30-300 cpm	30-300 cpm
	Oscillation type	Type	Fixed stroke and variable frequency	Variable stroke and frequency - Inverse oscillation	Variable stroke and frequency - Inverse oscillation
	Negative strip %	%	Fixed, -9	Variable	Variable
	Negative strip time	sec	Variable -0.08-0.12	0.12	0.09 - 0.11
Withdrawal Unit	Withdrawal	Type	Top & Bottom roll driven	Top & Bottom roll driven	Top & Bottom roll driven
	Straightener	Type	No drive	Top roll driven	Top roll driven
	Aux. Withdrawal	Y/N	Top roll driven	-	-
	Withdrawal Pressure (dummy bar/ strand)	bar			
	Drive	type	Cardon shaft	Chainless	Cardon Shaft
Spray Cooling	Type	Spray/mist	Water spray	Water spray	Water spray
	Dynamic / Manual	Type	Dynamic	Dynamic	Dynamic
	Zones	No.	3	4	4
EMS	Type	Mould/ strand / final	Mould EMS	Mould EMS	Mould & Final EMS
	Make	Make	Concast	DG	ABB
	Max current	Amp	400	400	400
	Frequency	Hz	3 – 7	3.5 - 7	3.5 - 5.5
	Location (zone of max gauss)	mm, from top of copper tube	300 (up position) 450 (down position)	600	700
	Poles	nos	6	6	6

3.3 Moulds used at CC3 in LD#1

Different moulds used at CC3 are as follows:

- Concast Convex
- Concast Convex-2
- Europa Metalli (without AMLC slot)
- Europa Metalli (with AMLC slot)
- Chetsu

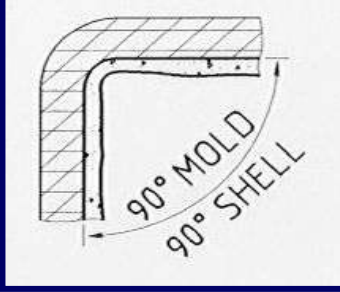
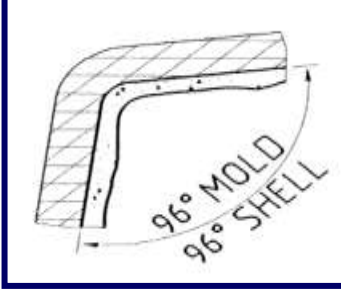
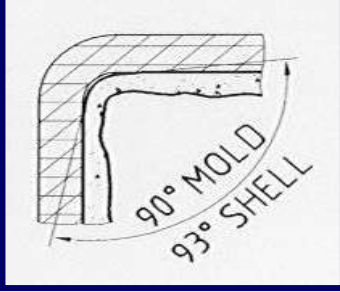
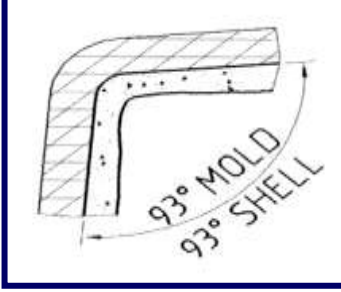
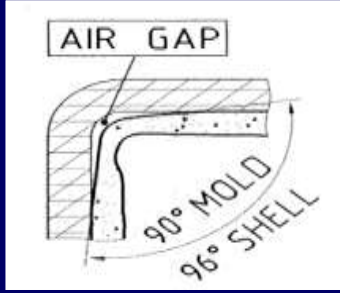
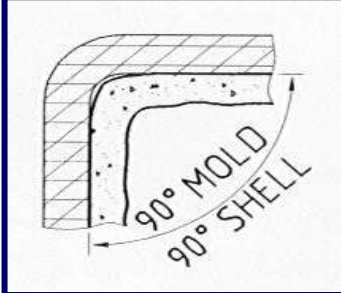
Table 3.2: Different Moulds used at CC3, LD#1

Mould types	AMLC Slot	Design/ Taper	Material	Coating
Europa Metalli	Yes	Parabolic taper,	Cu-Ag	Cr – 0.1mm
Europa Metalli	No	Parabolic taper	Cu-Ag	Cr – 0.1mm
Chuetsu	Yes	Parabolic taper	Cu- Cr-Zr	Cr – 0.1mm
Convex 2	Yes	Parabolic taper superimposed with convexity	Cu-Ag	Cr – 0.1mm
Convex	Yes	Parabolic taper superimposed with different convexity	Cu-Ag	Cr – 0.1mm

Among these Convex and Convex-2 are mainly used. The Convex mould design provides the most efficient heat transfer for billets.

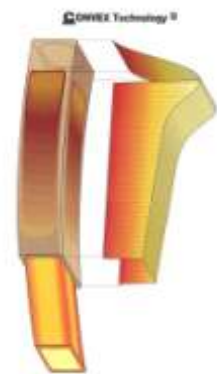
3.3.1 Comparison of Conventional and Convex Moulds

Table 3.3: Comparison of Conventional and Convex Moulds

CONVENTIONAL MOULD		CONVEX MOULD	
	<p>Heat transfer rapidly produces solid shell</p> <ul style="list-style-type: none"> ▪ Mould corner angle 90° ▪ Shell corner angle 90° 	<p>Heat transfer rapidly produces solid shell</p> <ul style="list-style-type: none"> ▪ Mould corner angle 96° ▪ Shell corner angle 96° 	
	<p>The corners contract away from the mould: heat transfer is retarded</p> <ul style="list-style-type: none"> ▪ Mould corner angle 90° ▪ Shell corner angle 93° 	<p>Change of mould geometry compensates corner shrinkage. The shell grows uniformly.</p> <ul style="list-style-type: none"> ▪ Mould corner angle 93° ▪ Shell corner angle 93° 	
	<p>Shell growth continues; re-melting takes place in the corners</p> <ul style="list-style-type: none"> ▪ Mould corner angle 90° ▪ Shell corner angle 96° 	<p>Corner air gap is minimal. Uniform shell thickness and even temperature</p> <ul style="list-style-type: none"> ▪ Mould corner angle 90° ▪ Shell corner angle 90° 	



Formation of air gap causes less heat transfer



Heat transfer is increased as the air gap formation is eliminated

3.3.2 Convex Type Mould

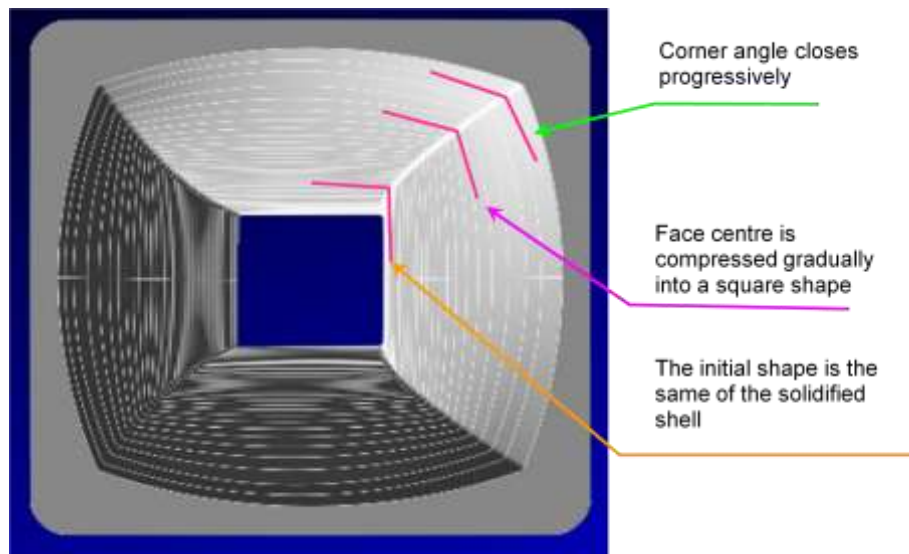
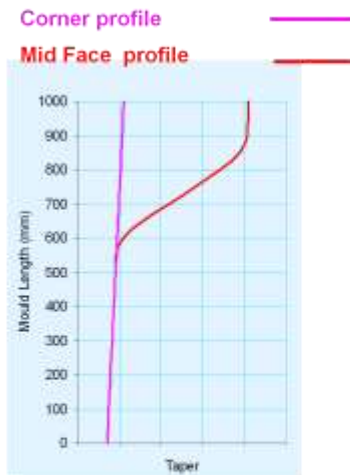
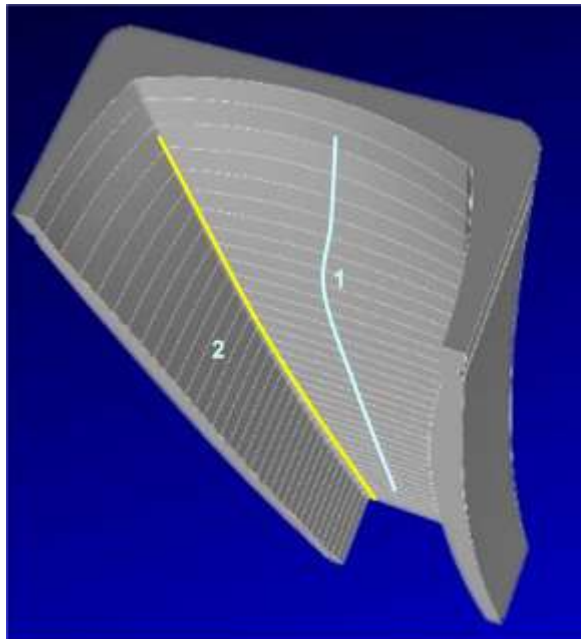


Fig.3.2: Top view of Convex type mould



- Changing shape of cavity maintains contact throughout the length of the mould tube
- Transition from Convex to straight tapered area generates billet shape at mould exit
- Gentle compression applied to mid-face of shell ensures good contact between strand and mould

Fig.3.2: Longitudinal view of Convex type mould and it's taper at both midface and corner

SCOPE AND OBJECTIVES

The main purpose of the organization is to produce quality billets which are as good as in quality and to produce it in the most economical way with optimum conditions during manufacture. During continuous casting of the billets there are many problem arises out of which mould is one of the most important part. After reviewing the literature critically and studying the effect of rhomboidity over consequent rolling operations, the scope of the problem and the objectives of the present study have been formulated which are as follows:

1. To ascertain if there is any relationship between casting speed, superheat and rhomboidity (for both moulds: Convex and Convex-2).
2. In case a relationship exists, then specify safe working ranges.
3. To study and compare the solid shell formation of in both Convex and Convex-2 moulds used at CC3, LD#1.

EXPERIMENTAL SETUP AND PROCEDURE

As a part of the study of effects of casting speed, superheat and mould over rhomboidity, trails were conducted at CC3, LD#1. The details of data analysis and trails will be presented in this chapter.

5.1 Casting Machine and Operating Practices

CC3 is a six strand billet caster producing 130 x 130 mm² billets of various grades of steel, mainly TMT grade. The trails were conducted on the first and the sixth strand of the caster. Two different kind of mould were used at CC3 which were manufactured by Concast – Convex and Convex-2 with initial taper of 3.8%/m and 2.3%/m respectively in a 9 m radius curved mould machine. The mould was oil lubricated and had sinusoidal oscillation. The tundish capacity was 30 tins and was delta type with a pour pad and no internal furniture. The casting speed was varied from 2.8 to 4.0 m/min through a change in tundish weight, and/or change in tundish nozzle diameter. The specifications of the casting machine are given in Table 3.1.

5.1.1 Experimental Casting Parameters

The experimental variable included casting speed, superheat and mould type. These variables were monitored for Fe 500D (TMT) grade of steel. Effect of casting speed and superheat was analysed from the data obtained for 6 months (September'11 to February'12). Casting speed was taken as the average casting speed over one heat strand wise. The data were collected from Level-2 of LD#1 Automation.

5.2 Details of Plant Trail

From literature findings it is clear that mould is mainly responsible for rhomboidity. Various mould related parameters affect the severity of rhomboidity. Solid shell formation is a very important aspect as uneven shell thickness leads to shape defects in billets. To understand the behavior of shell formation in the mould, plant trails were conducted at CC3, LD#1.

The trails involve following steps:

- FeS powder was inserted into the mould of strand in the last billet to be cast at the end of a sequence.
- CNC was fired after ten seconds.
- After the withdrawal, billet was marked by chalk for proper identification.
- 2 m length was gas cut from 0.5 m from the tail end.
- The section was gas cut into 20 pieces of approx. 100 mm each.
- From each piece 50 mm sample was to be cut and grinded on both the transverse faces.
- Sulphur print was obtained for these faces for all 20 samples.

The trail was carried out for two heats. The details of the trails are mentioned in Table 5.1.

Table 5.1: Plant Trail Details

	TRAIL 1	TRAIL 2
Heat No.	M00983	M01820
Grade	Fe 500D	Fe 500D
Section (mm ²)	130 x 130	130 x 130
Casting Speed (m/min)	3.2	3.1
Carbon (wt.%)	0.22	0.213
Superheat (°C)	24°C	30°C
Strand Number	6	1
Mould Type	Convex	Convex-2

FeS when introduced to the mould would penetrate the liquid core up to one meter. There will be instantaneous dissolution of powder due to its small size (< 200 mesh number). The Solid shell already formed prior to the addition of FeS would not have sulphur content as FeS would not be able to dissolve in the solid shell. Taking sulphur print of the experimented billet will give white band in the periphery of the billet representing the solid shell already formed.

5.3 Billet Sample Preparation

The gas cut samples of both trial billets were taken to Physical Laboratory, Scientific Services for surface preparation. A 50 mm sample was cut from each 100 mm sample and the both transverse faces of the 50 mm sample were grinded.

5.4 Sulphur Printing (Baumann Method)

The sulphur printing was carried out at Metallography Laboratory, Scientific Services. FeS powder under 200 mesh size was prepared by pulverising FeS cylinders of 10mm diameter and 10 mm height in pulverizer at Mineral Beneficiation Laboratory at R&D.

5.4.1 Principle

The Baumann method for the macrographic examination of steel by sulphur printing is a qualitative test which is employed to detect the distribution of sulphur in steel and certain physical irregularities, such as cracks and porosity, by printing on photo-sensitive paper previously soaked in sulphuric acid. Here sulphur printing has been carried out to measure the solid shell thickness in the mould. As sulphur will not dissolve in solid shell formed, it will give a white band on the printing which represents shell thickness.

5.4.2 Procedure

A shallow container, such as photographic tray, is required to contain the sulphuric acid solution. The container should be large enough to soak the photographic paper without excessive folding of the paper. A similar tray is required to hold the photographic fixing solution, such as sodium hyposulphite in our case.

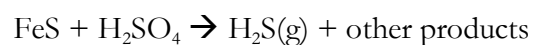
The photographic paper is silver bromide paper. After soaking the paper for 10 minutes in sulphuric acid solution, the damp sensitive side of the paper is applied to the surface to be examined. To ensure good contact, eliminate air bubbles and drop of liquid between the surfaces of the test piece and sheet of paper, for example by means of a rubber roller. This should be done carefully so that the paper does not slip. The photographic paper is allowed to remain in contact with the test surface for 5 minutes.

The printed sheet is then carefully peeled off and washed in running water for 2-3 minutes.

The print is then immersed in a fixing solution (sodium hyposulphite) for another 5 minutes, and then it is washed for 5 minutes under running water and left for drying for at least 30 minutes.

The procedure should be carried out in a dark room to avoid any affect of the ambient light.

The chemical reactions during sulphur printing are as follows:



5.5 Plant Trail Difficulties

During conducting trails, following were the difficulties faced:

- Stamping of strand numbers was poor, causing difficulties in billet identification strandwise.
- No proper mechanism of introducing FeS powder into the metal stream pouring into the mould.
- Tracing of the billet section containing FeS after complete solidification was difficult. Estimation was used to mark the required section.

RESULTS AND DISCUSSION

This chapter contains the discussion on the results obtained from data analysis and plant trails.

6.1 Effect of Casting Speed on Rhomboidity

Data for 6 months period (September 2011 to February 2012) was collected from Level 2 Automation at LD#1. The data were filtered for 'TMT' grade at CC3. Strandwise analysis was carried out for the effect of casting speed on rhomboidity. The casting speed taken here is the average casting speed over a heat.

Figures 6.1 to 6.6 represent the severity of diagonal difference over various casting speeds.

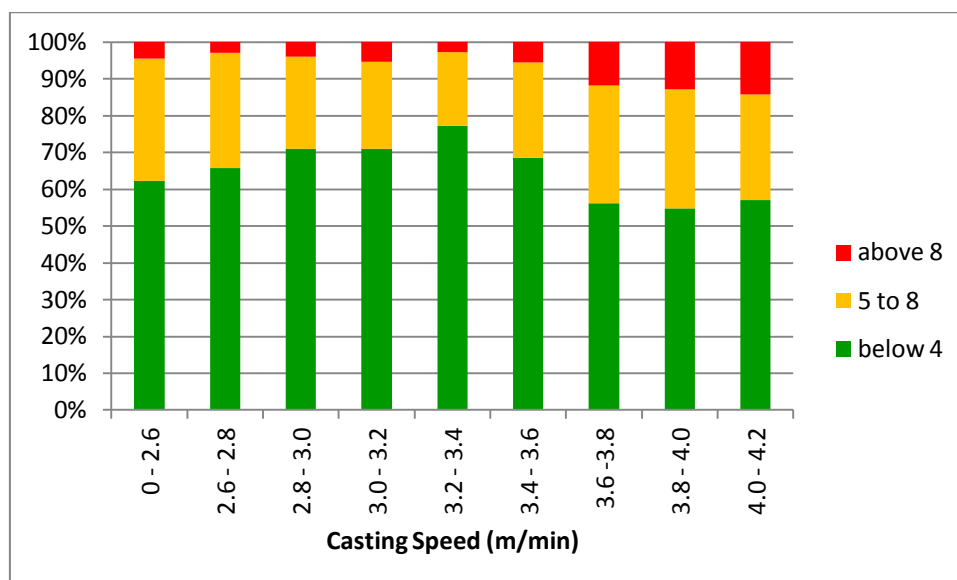


Fig.6.1: Variation in rhomboidity with casting speed for Strand 1 at CC3

Table 6.1: Casting speed and rhomboidity for Strand 1

Casting Speed (m/min)	Number of Billets		
	Below 4 mm	Between 5 to 8 mm	Above 8 mm
0 - 2.6	28	15	2
2.6 - 2.8	23	11	1
2.8 - 3.0	54	19	3
3.0 - 3.2	66	22	5
3.2 - 3.4	142	37	5
3.4 - 3.6	211	80	17
3.6 - 3.8	95	54	20
3.8 - 4.0	17	10	4
4.0 - 4.2	4	2	1

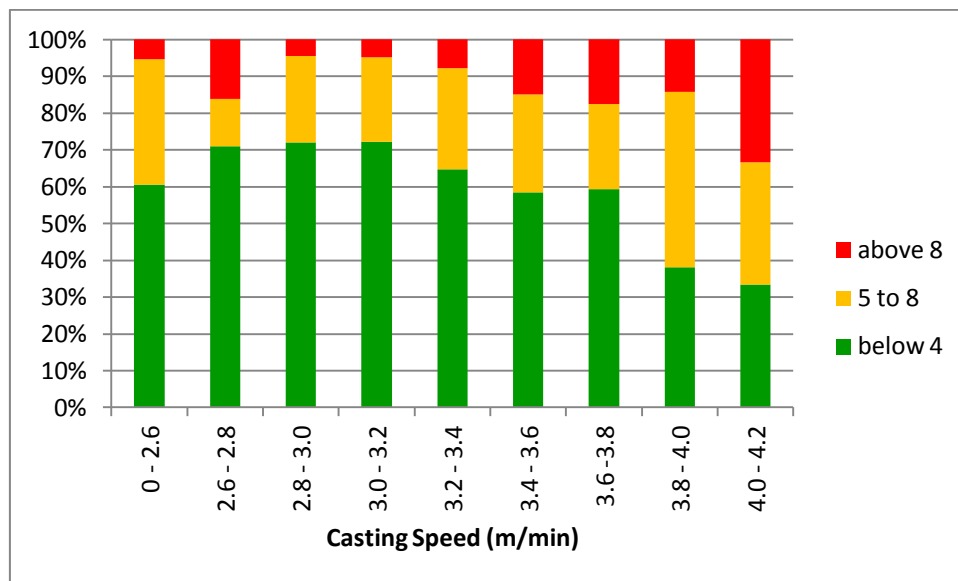


Fig.6.2: Variation in rhomboidity with casting speed for Strand 2 at CC3

Table 6.2: Casting speed and rhomboidity for Strand 2

Casting Speed (m/min)	Number of Billets		
	Below 4 mm	Between 5 to 8 mm	Above 8 mm
0 - 2.6	23	13	2
2.6 - 2.8	22	4	5
2.8 - 3.0	49	16	3
3.0 - 3.2	91	29	6
3.2 - 3.4	167	71	20
3.4 - 3.6	189	86	48
3.6 - 3.8	64	25	19
3.8 - 4.0	8	10	3
4.0 - 4.2	1	1	1

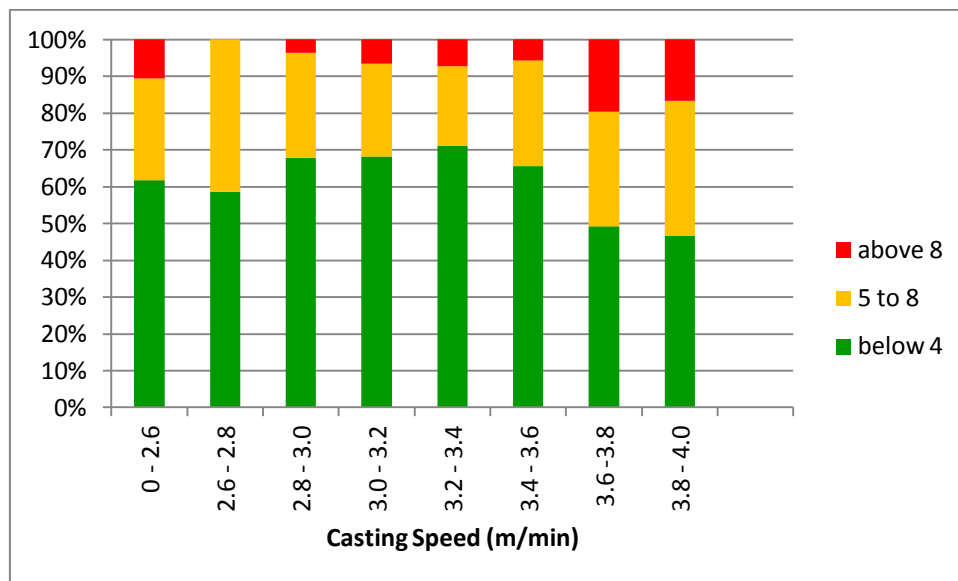


Fig.6.3: Variation in rhomboidity with casting speed for Strand 3 at CC3

Table 6.3: Casting speed and rhomboidity for Strand 3

Casting Speed (m/min)	Number of Billets		
	Below 4 mm	Between 5 to 8 mm	Above 8 mm
0 - 2.6	29	13	5
2.6 - 2.8	17	12	0
2.8 - 3.0	38	16	2
3.0 - 3.2	62	23	6
3.2 - 3.4	188	57	19
3.4 - 3.6	199	87	17
3.6 -3.8	68	43	27
3.8 - 4.0	14	11	5

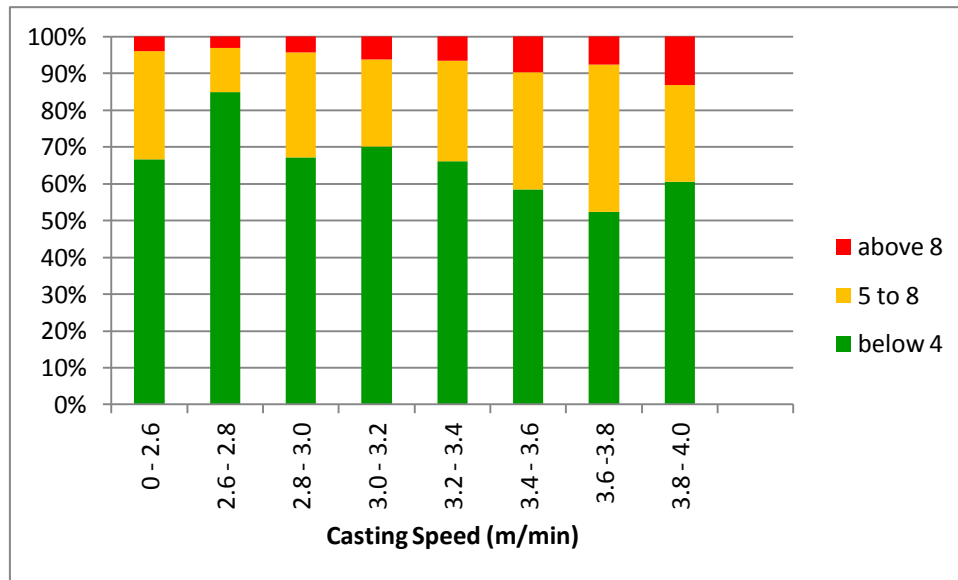


Fig.6.4: Variation in rhomboidity with casting speed for Strand 4 at CC3

Table 6.4: Casting speed and rhomboidity for Strand 4

Casting Speed (m/min)	Number of Billets		
	Below 4 mm	Between 5 to 8 mm	Above 8 mm
0 - 2.6	34	15	2
2.6 - 2.8	28	4	1
2.8 - 3.0	47	20	3
3.0 - 3.2	68	23	6
3.2 - 3.4	150	62	15
3.4 - 3.6	181	99	30
3.6 -3.8	55	42	8
3.8 - 4.0	23	10	5

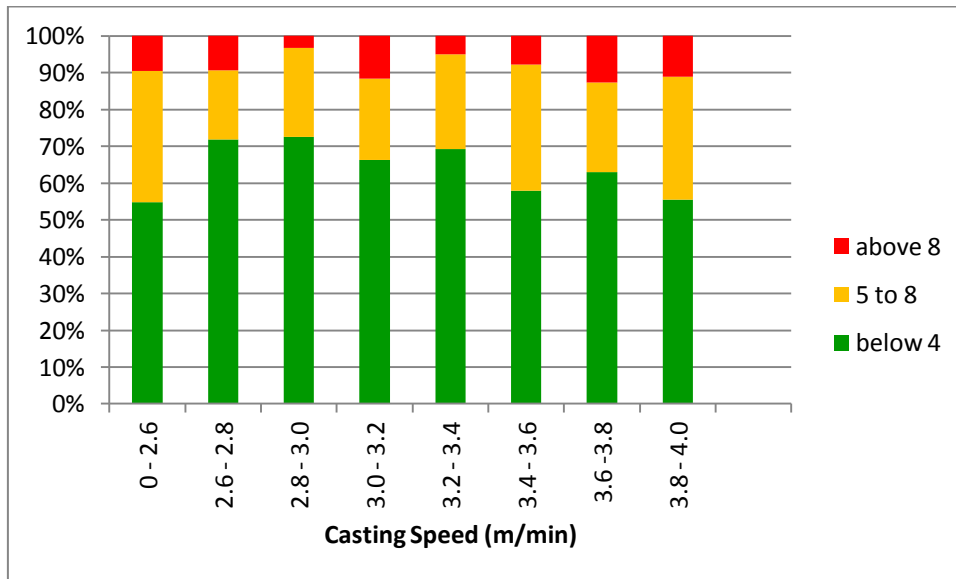


Fig.6.5: Variation in rhomboidity with casting speed for Strand 5 at CC3

Table 6.5: Casting speed and rhomboidity for Strand 5

Casting Speed (m/min)	Number of Billets		
	Below 4 mm	Between 5 to 8 mm	Above 8 mm
0 - 2.6	23	15	4
2.6 - 2.8	23	6	3
2.8 - 3.0	45	15	2
3.0 - 3.2	57	19	10
3.2 - 3.4	166	62	12
3.4 - 3.6	192	113	26
3.6 -3.8	90	35	18
3.8 - 4.0	10	6	2

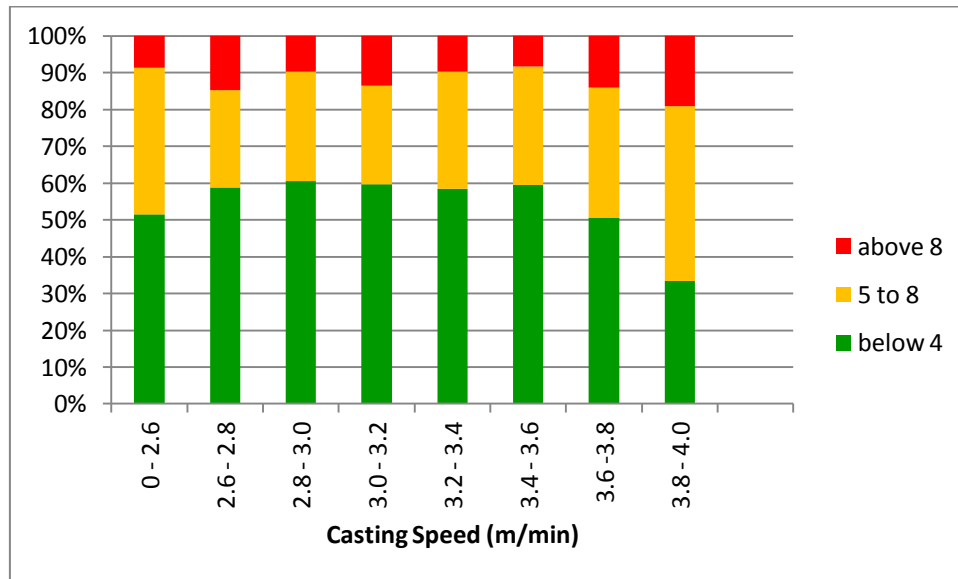


Fig.6.6: Variation in rhomboidity with casting speed for Strand 6 at CC3

Table 6.6: Casting speed and rhomboidity for Strand 6

Casting Speed (m/min)	Number of Billets		
	Below 4 mm	Between 5 to 8 mm	Above 8 mm
0 - 2.6	18	14	3
2.6 - 2.8	20	9	5
2.8 - 3.0	69	34	11
3.0 - 3.2	93	42	21
3.2 - 3.4	138	75	23
3.4 - 3.6	115	62	16
3.6 -3.8	36	25	10
3.8 - 4.0	7	10	4

From the above graphs (Figures 6.1 to 6.6), a trend is shown represent increase in percentage cases of rhomboidity as the casting speed is increased. From the literature it is a well known that with increase in casting speed, the heat transfer also increases resulting in thinner shell thickness at the mould exit, due to decreased residence time of the strand in the mould. These thin shells are weak, and poor control of process, such as metal level control and non uniform cooling of the strand can lead to rhomboid billets. Therefore, a viable shell thickness is required at the entry into the spray chamber to ensure that the unsupported strand can withstand the ferrostatic pressure of the liquid core and the thermo-mechanical stresses.

6.2 Effect of Superheat on Rhomboidity

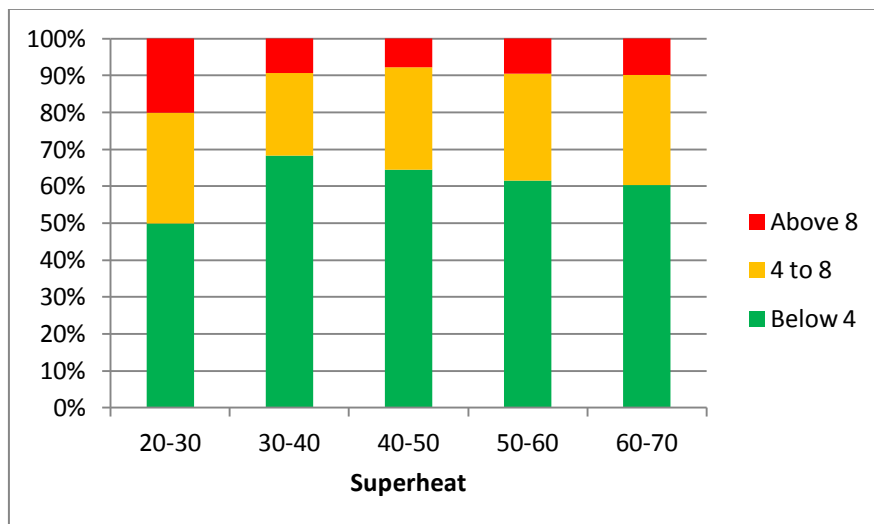
**Fig.6.7:** Variation in rhomboidity with different ranges of superheat at CC3

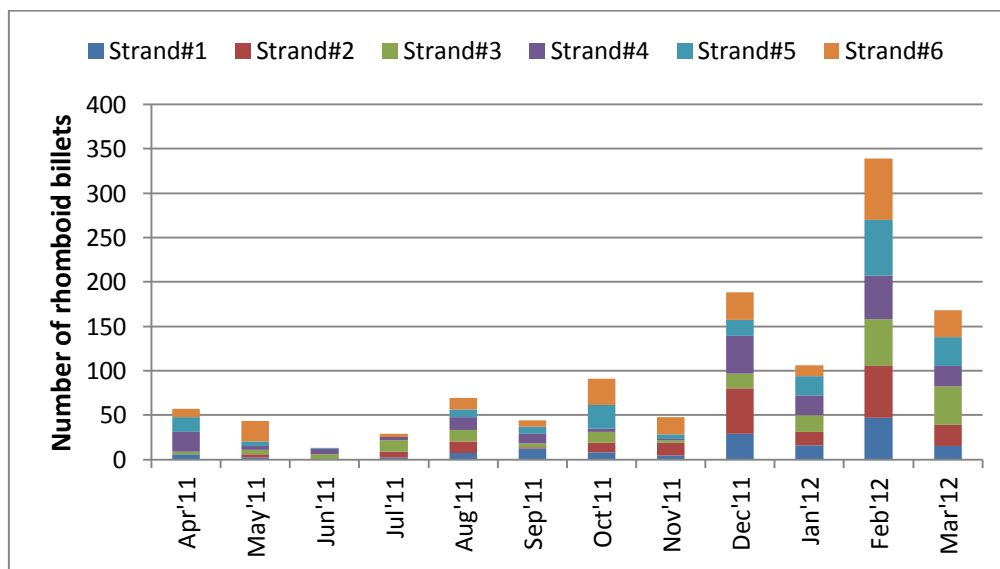
Table 6.7: Superheat and rhomboidity for CC3

Superheat (°C)	Number of Billets		
	Below 4 mm	Between 5 to 8 mm	Above 8 mm
20-30	15	9	6
30-40	242	79	33
40-50	955	413	114
50-60	580	273	89
60-70	134	66	22
70-80	20	10	0
80-90	3	3	0

No specific pattern is revealed of the effect of superheat on rhomboidity. Higher superheat increases the strand temperature, delaying the onset of solidification at the meniscus. This increased billet surface temperature results in thinner shell formation with lower tensile strength leading to surface defects and even rupture.

6.3 Effect of Mould on Rhomboidity

Total numbers of cases of rhomboidity were found in CC3 during the period of April 2011 to March 2012, as shown in Figure 6.8. From October 2011 onwards it was observed that the cases of rhomboidity had a considerable increase. On further investigation it was found that Convex-2 type of mould was being supplied by Concast instead of Convex type. Months of December'11 to March'12 have very high number of rhomboid billets as Convex-2 mould was used most of the time, especially in February'12. Causes of rhomboidity due to Convex-2 mould was then studied which has been discussed in the later section 6.3.1 and 6.3.2.

**Fig.6.8:** Number of rhomboid billets from CC3 in FY 2011-12 (strandwise)

6.3.1 Mould Taper and Section Size

Mould taper and section size was measured by Concast MCS-3000 (Mould Control System). Figure 6.9, show the taper and wall to wall distance between the midfaces on the curved side for both Convex and Convex-2 type.

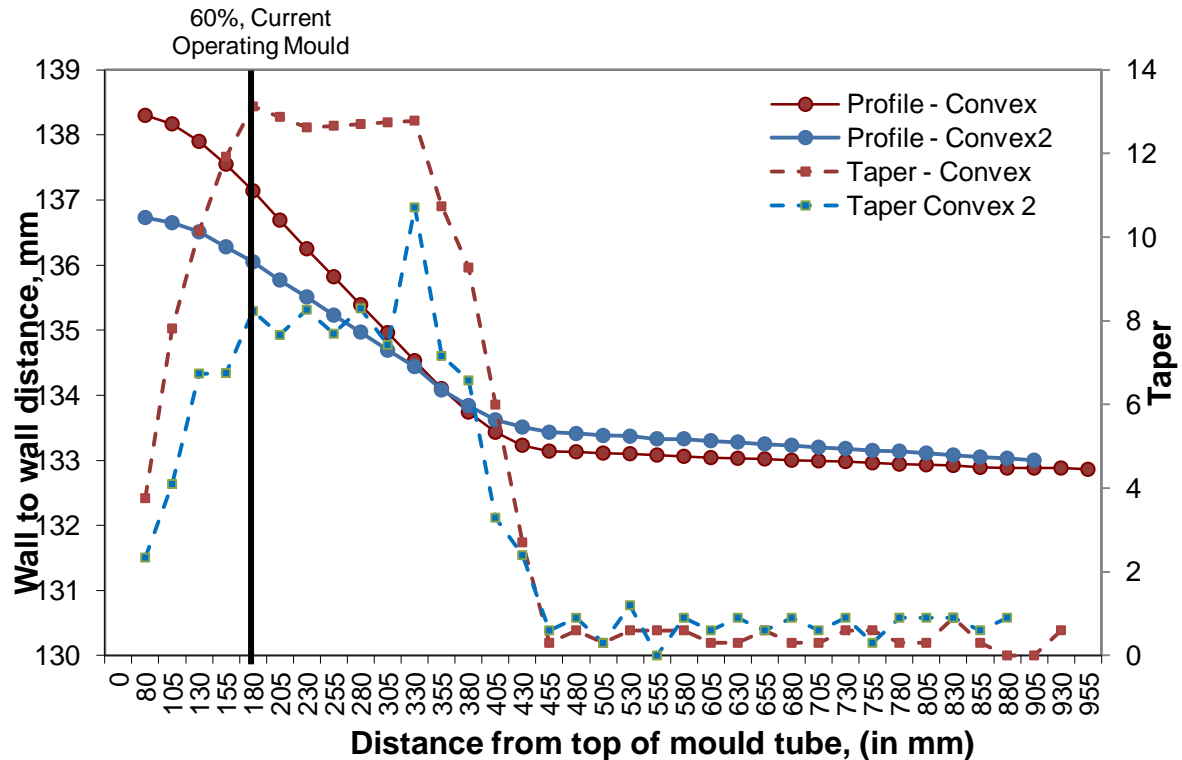


Fig.6.9: Mould profile and taper of curved side for Convex and Convex-2 moulds

From the taper profile of Convex and Convex-2 type of moulds, it can be suggested that the rhomboidity is less of a problem in operations employing steep mould tapers in the meniscus region, as in the case of Convex mould. It is quite possible that the role of mould taper on severity of rhomboidity is linked to its strong effect on mould heat extraction and therefore, to the mould hot-face temperature.

The dynamic taper of steeper mould would cause interference between the strand and the oscillation. In particular, during the upstroke cycle of mould oscillation, a great deal of mechanical interaction would occur between steep dynamic taper and the solidifying strand, resulting in high heat transfer at the meniscus level.

6.3.2 Solid Shell Formation in Convex and Convex-2 Type Mould

Understanding of solid shell formation inside the mould is one of the key issues in understanding the root cause of rhomboidity. Most of the researchers are of the opinion that rhomboidity is generated in the mould itself which is later enhanced in the secondary cooling stage.

For getting solid shell thickness inside the mould, sulphur print technique was used by adding extra sulphur in form FeS in the mould itself during casting.

Figures 6.10(a to n) represents sulphur prints of billet casted by Convex-2 mould at different distances from the mould entry.

6.3.2.1 Sulphur Prints for Billet Cast by Covex-2 Mould



Fig.6.10(a): D = 180 mm

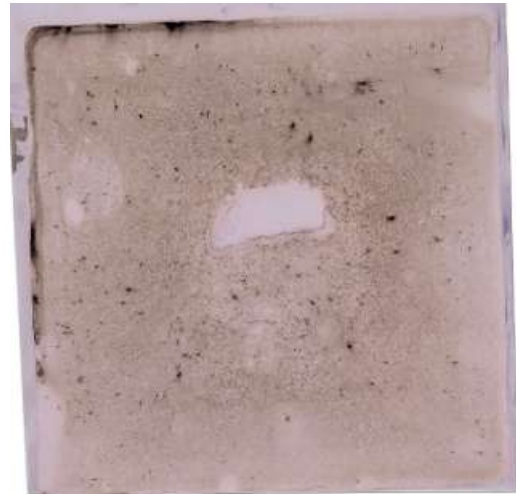


Fig.6.10(b): D = 230 mm



Fig.6.10(c): D = 300 mm



Fig.6.10(d): D = 350 mm



Fig.6.10(e): $D = 410$ mm

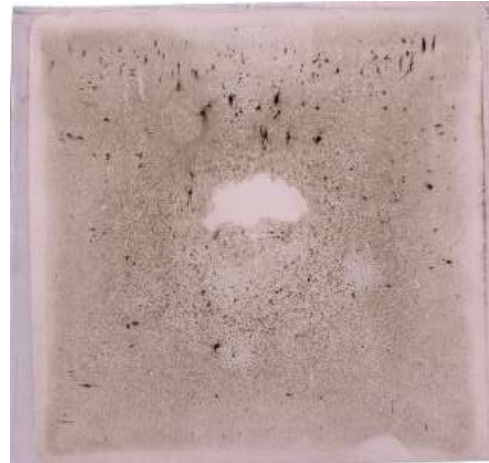


Fig.6.10(f): $D = 460$ mm

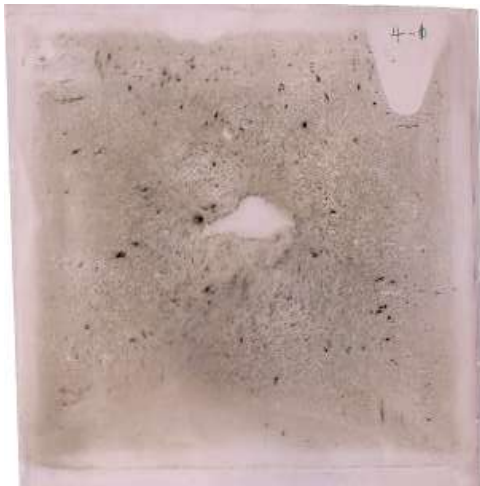


Fig.6.10(g): $D = 500$ mm



Fig.6.10(h): $D = 550$ mm



Fig.6.10(i): $D = 620$ mm



Fig.6.10(j): $D = 660$ mm



Fig.6.10(k): D = 700 mm



Fig.6.10(l): D = 760 mm



Fig.6.10(m): D = 810 mm



Fig.6.10(n): D = 860 mm

6.3.2.2 Sulphur Prints for Billet Cast by Convex Mould



Fig.6.11(a): D = 180 mm

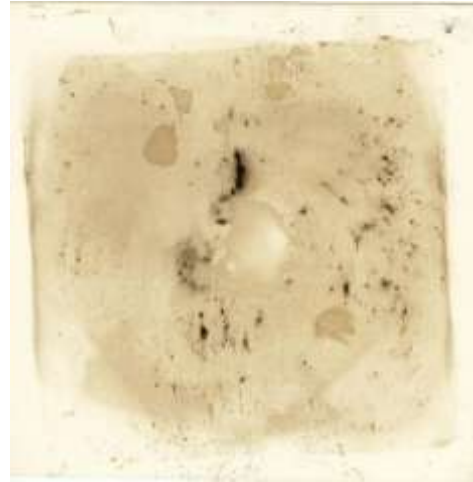


Fig.6.11(b): D = 230 mm



Fig.6.11(c): D = 300 mm



Fig.6.11(d): D = 350 mm

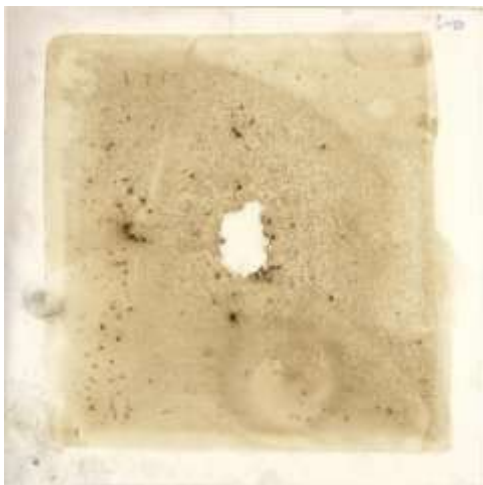


Fig.6.11(e): D = 410 mm



Fig.6.11(f): D = 460 mm

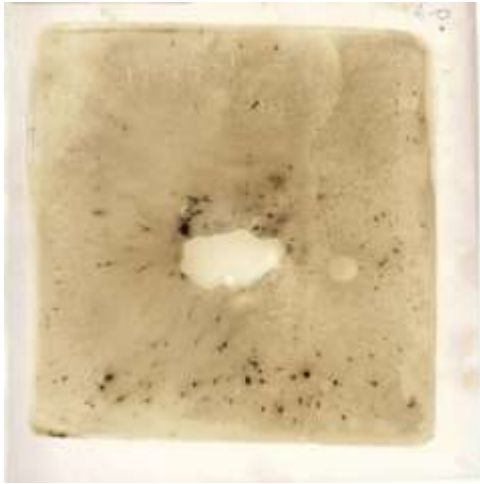


Fig.6.11(g): $D = 500 \text{ mm}$



Fig.6.11(h): $D = 550 \text{ mm}$



Fig.6.11(i): $D = 620 \text{ mm}$

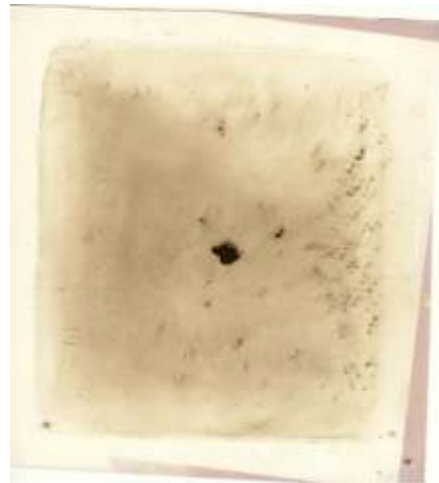


Fig.6.11(j): $D = 680 \text{ mm}$

Figures 6.11(a to j) represents sulphur prints of billet casted by Convex mould at different distances from the mould entry

6.3.2.3 Solid Shell Comparison for Convex and Convex-2 Mould

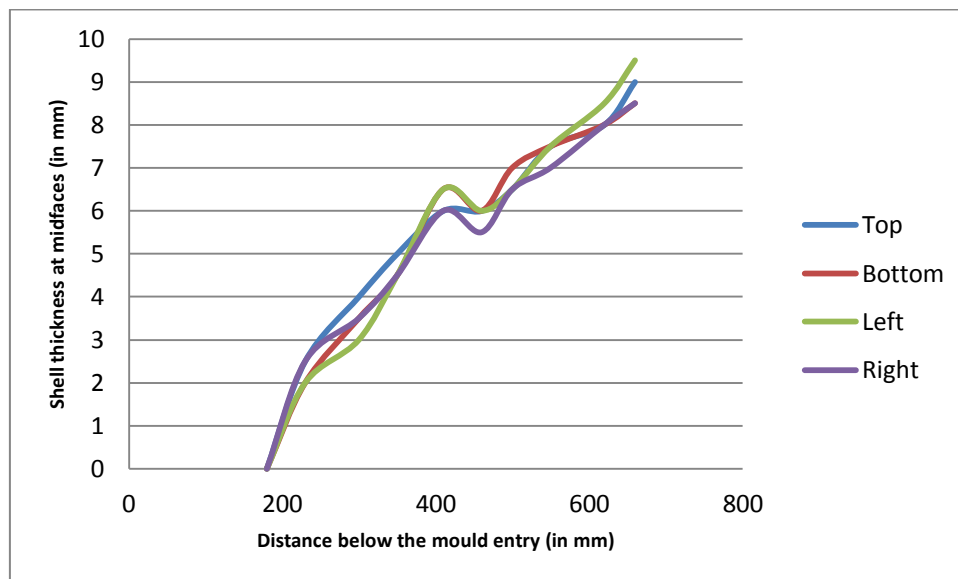


Fig.6.12: Solid shell formation profile for midfaces of Convex mould on curved side

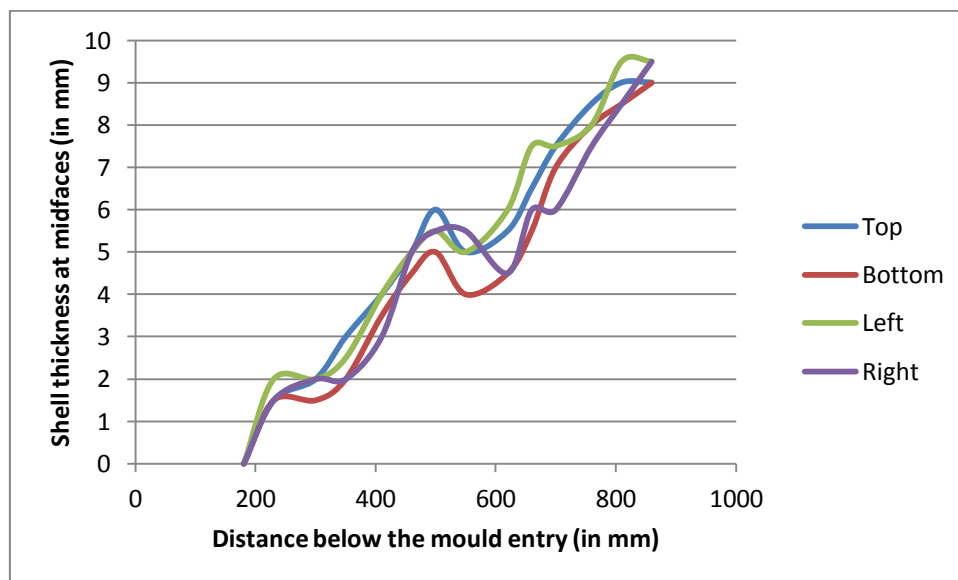


Fig.6.13: Solid shell formation profile for midfaces of Convex-2 mould on curved side

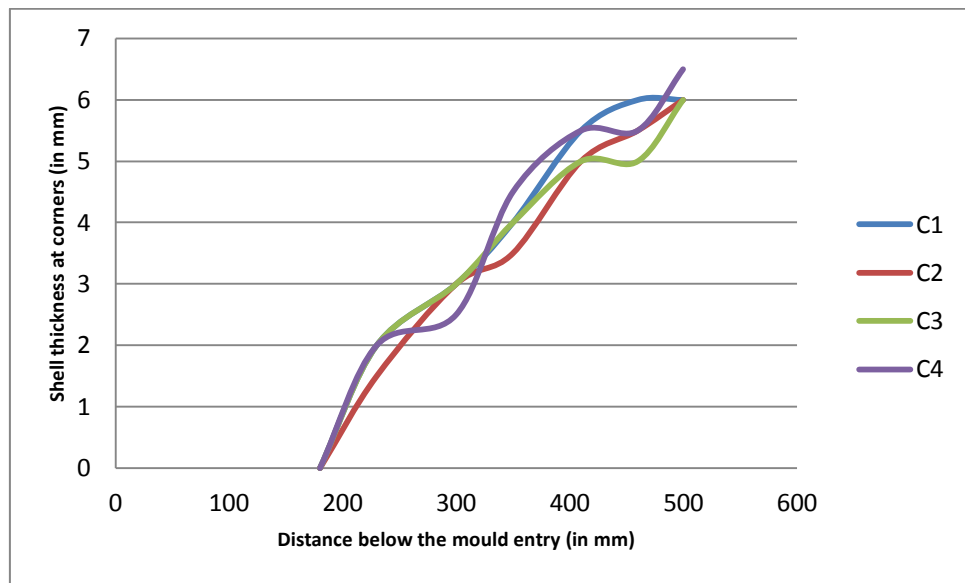


Fig.6.14: Solid shell formation profile for corners of Convex mould on curved side

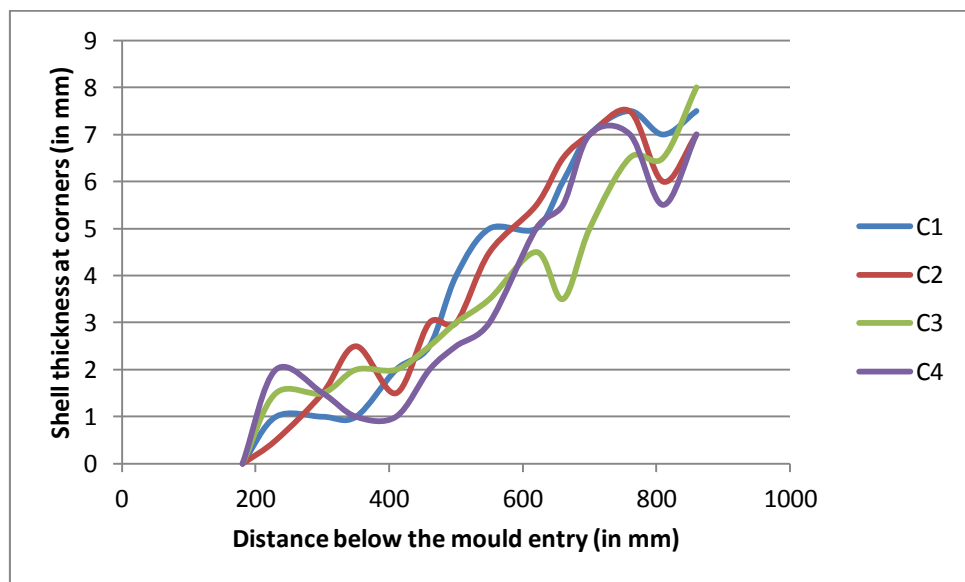


Fig.6.15: Solid shell formation profile for corners of Convex-2 mould on curved side

From the Figures 6.12 and 6.13, it can be suggested that shell thickness at the midfaces in Convex mould are thicker and much uniform than in case of Convex-2 mould. A drop in shell thickness is observed in both the cases in 500 – 700 mm range. This may be because of the presence of MEMS (Mould Electromagnetic Stirrer) which may be causing re-melting of the solid shell.

From the Figures 6.14 and 6.15, it can be suggested that shell thickness at the corners in Convex mould are thicker and cases of re-entrant corners are very less than in case of Convex-2 mould. Moreover, it is very clear that shell thickness at the corner is also higher for Convex mould. In Figure 6.15, corner shell thickness reduces at some areas which is due to the formation of re-entrant corners and hence it can be safely stated that air gap formation in Convex-2 mould is significant.

6.4 Mechanism of Generation of Rhomboidity

From the results obtained above, non-uniform solid shell thickness plays an important role in generation of rhomboidity, especially the shell thickness at the corners. Considering a case of non-uniform solid shell, in which shell thickness at one corner is thick and at the adjacent corner is thin. There will be high compressive stresses over the outer face of the strand at the corner and low tensile stresses over inner face adjacent to liquid core, whereas, there will be low compressive stresses over the outer face and high tensile stresses over the inner surface of the thinner corner, as shown in Figure 6.16.

The resultant stresses over thicker corners cause it to shrink to an acute angle whereas the thinner shell corner will lead to obtuse corner formation. Corner act as a hinge for the adjacent faces, so in case of low corner shell thickness, a square billet will shear to form a rhomboid billet.

At the mould exit, the billet cannot be rhomboid but due to variable shell thickness rhomboidity is exhibited by aid of secondary cooling. The genesis of the rhomboidity problem lies in the mould which then is enhanced by secondary cooling.

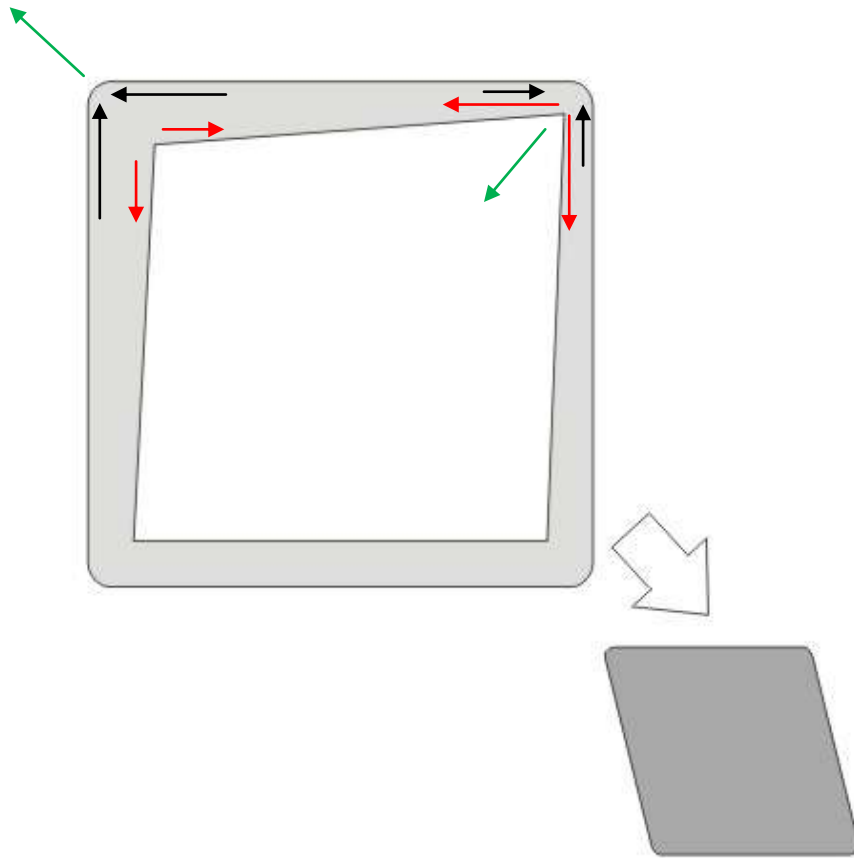


Fig.6.16: Stress distribution over adjacent corners with thick and thin shell which leads to rhomboid billet. The red arrow represents tensile stress while black represent compressive stress and green arrow represent the resultant stress at both corners.

CONCLUSIONS

After detailed analysis of results the following conclusions were reached upon:-

- With increase in casting speed, probability of rhomboidity occurrence in billets increases.
- Superheat has no particular effect on rhomboidity as latent heat forms 95% of the amount of heat being extracted.
- Convex mould is more effective in controlling rhomboidity than Convex-2 mould.
- The steeper taper in Convex mould helps in thicker solid shell formation in the mould.
- The corner shell thickness is more in case of Convex mould.
- The formation of re-entrant corners is less in Convex mould suggesting less air gap formation.
- Convex type mould gives a better performance in terms of rhomboidity.

WAY FORWARD

- Conduct plant trials with varying casting speeds and for different grades and carry out their sulphur print in the similar manner as presented in this study.
- Development of stress model for billet solidification in order to analyse the proposed mechanism of rhomboidity.
- Casting of plaster of paris inside the Convex and Convex-2 mould in order to perform detailed study over the mould profile, taper and corner angles.

REFERENCES

- [1] J.K. Brimacombe, I.V. Samarasekera, and J.E. Lait: "Continuous Casting Vol. 2 Heat Flow, Solidification and Crack Formation," ISS-AIME, 1984.
- [2] J.K. Brimacombe: "Empowerment with Knowledge – Toward the Intelligent Mold for the Continuous Casting of Steel Billets", Metallurgical Transactions B, 1993, Vol. 24B, No.6, pp. 917-935.
- [3] I.V. Samarasekera: "Thermal Distortion of Continuous Casting Moulds", Ph.D Thesis, The University of British Columbia, Canada, 1980.
- [4] S.Kumar, I.V. Samarasekera, and J.K. Brimacombe: "Mould Thermal Response and Formation of Defect in the Continuous Casting of Steel Billets. Part I. Formation of Laps and Bleeds", ISS Transactions, June 1997, pp. 51-67.
- [5] I.V. Samarasekera, and J.K. Brimacombe: "Thermal and Mechanical Behaviour of Continuous Casting Billet Moulds", Ironmaking and Steelmaking, 1982, Vol. 9, pp. 1-15.
- [6] S. Chandra: "Heat Transfer, Oil Lubrication and Mould Taper in Steel Billet Casting Machines", Ph.D Thesis, The University of British Columbia, Canada, 1992.
- [7] C. Chow: "The Effects of High Casting Speed Casting on the Mould Heat Transfer, Billet Solidification, and Mould Taper Design on Continuously Cast Steel billets", Ph.D Thesis, The University of British Columbia, Canada, 1999.
- [8] I.V. Samarasekera, and J.K. Brimacombe, 2nd Process Technology Conference - AIME, 1981, Vol. 2, pp. 2-21.
- [9] S.Kumar, I.V. Samarasekera, and J.K. Brimacombe: "Mould Thermal Response and Formation of Defect in the Continuous Casting of Steel Billets. Part II. Rhomboidity", ISS Transactions, December 1998, pp. 51-66.
- [10] S.N. Singh and K.E. Blazek: "Open Hearth Proceedings- AIME", 1975, Vol. 60, pp. 16-36.
- [11] A. Grill and J.K. Brimacombe: Ironmaking and Steelmaking, 1976, Vol. 3, No. 2, pp.76-79.

- [12] J.E. Lait, J.K Brimacombe and F. Weinberg: Iron and Steelmaking, 1974, Vol. 3, No. 2, pp.35-42.
- [13] R. Bommaraju I.V. Samarasekera, and J.K. Brimacombe: "Mould Thermal Response and Formation of Defect in the Continous Casting of Steel Billets. Part III. Structure, Solidification Band, Crack Formation and Off-Squarness", ISS Transactions, 1984, Vol. 5, pp. 51-66.